# EN-ROUTE AIR TRAFFIC OPTIMIZATION UNDER NOMINAL OR PERTURBED CONDITIONS, ON A 3D DATA-BASED NETWORK FLOW MODEL

A Thesis
Presented to
The Academic Faculty

by

Aude Marzuoli

In Partial Fulfillment
of the Requirements for the Degree
Master in the
School of Aerospace Engineering

Georgia Institute of Technology
May 2012

# EN-ROUTE AIR TRAFFIC OPTIMIZATION UNDER NOMINAL OR PERTURBED CONDITIONS, ON A 3D DATA-BASED NETWORK FLOW MODEL

Approved by:

Professor Eric Feron, Committee Chair
School of Aerospace Engineering
Georgia Institute of Technology

Professor Amy Pritchett
School of Aerospace Engineering
Georgia Institute of Technology

ProfessorJ.-P. Clarke
School of Aerospace Engineering
Georgia Institute of Technology

Dr Maxime Gariel

Rockwell Collins

Date Approved: February 20, 2012

*To my family,*

*Aude*

# ACKNOWLEDGEMENTS

I would like to thank Eric Feron for giving me the opportunity to work on a research project, and for his thoughtful pieces of advice. Thank you Eric for your support, especially when I was sick. I feel that I have learned a lot, and that made me all the more eager to learn more.

I would also like to thank Maxime Gariel, for being such a great mentor and guiding me patiently through my first steps here at Tech. I would like to thank Adan Vela for reviewing my papers endlessly and being a great person to discuss research issues with. I would like to thank Amy Pritchett and John-Paul Clarke for being on my thesis committee, for their advice, and for helping me make this thesis better. I would like to thank Liling Ren for providing results from his work at Tech.

I would like to gratefully acknowledge Dawn McIntosh and NASA (Grant NNX08AY52A), for sponsoring this thesis.

To my parents, my brother, and my grand parents, thank you for your love and support. To my friends, Ito, Eleonore, Romain, Tim, Timo, Vivek, Florian, Ben, thanks for making this time so memorable! To Manu, thanks for always being so great.

To the reader, thank you for reading these acknowledgments, and enjoy the thesis.

# TABLE OF CONTENTS

# LIST OF FIGURES

# CHAPTER I

# INTRODUCTION

## *1.1 Air traffic management*

In the coming decades, air traffic demand is expected to increase significantly. The present airspace capacity limits, i.e. the maximum number of aircraft allowed in a given airspace, are predicted to be exceeded in the coming years [25]. With congestion problems becoming more and more acute in many airports and air sectors, delays caused by congestion or weather perturbations are increasing, and so are the associated costs. Robust tools are needed to better manage congestion and delays by air traffic flow managers. These tools will come into effect under the 'paradigm shift', supported by innovative technologies [18].

The National Airspace System (NAS) is comprised of 21 Centers, each of which is divided into sectors. The current Enhanced Traffic Management System (ETMS) provides a congestion alerting function which uses peak-one minute aircraft count as a sector congestion alerting criterion (the Monitor Alert Parameter, or MAP). The MAP values used in current day operations are not optimized to consider weather disruptions and re-routing. In the NAS, the goal of en-route Traffic Flow Management (TFM) is to balance air traffic demand against available airspace capacity, in order to ensure a safe and expeditious flow of aircraft.

The Traffic Flow Management Problem aims at solving real and complex situations in air traffic. As Odoni points out in 1994, there is an imperative for the

resolution of the TFM problem [26]. In 1998, Bertsimas and Stock proposed a mathematical model for the TFM problem, showing both theoretical results and example applications [2]. Later in 2000, they presented a network flow approach to dynamically reroute aircraft [3]. This work was further deepened to cover all phases of flight and have the computational efficiency to solve problems of the size of the NAS [19]. Geng and Cheng addressed the TFM problem by developing a method based on integer programming in order to determine the temporal availability of routes during specific time intervals [12]. Dell'Olmo and Lulli [9] used a Free Flight scenario, using a network with no fixed routes, meaning that each aircraft could follow any link in the network, the goal being to arrive precisely in time at the destination. These works were concerned with scheduling issues, but did not take into account spatial interactions between aircraft. Some took into account airport departure and arrival capacities and air sector capacity, as deterministic functions of time, known in advance with certainty. They did not offer alternative route options for a given flight.

Air Traffic Flow Management is sensitive to changes in capacity. Daily operations in Air Traffic involve diverting flights, especially when the airspace is perturbed, because of congestion or weather disturbances. Various ways of responding to weather scenarios have been envisioned. Finding the best possible routes under weather to ensure safety and operations continuity is another vast area of research. Mitchell et al. use algorithms to compute geometric flow capacity in 2D and evaluate the capacity of an airspace having a deterministic set of weather constraints [24]. In [17], different algorithms to synthesize weather avoidance routes are presented and their advantages and drawbacks compared. Furthermore, research in Air Traffic Management has produced useful models to optimize traffic, showing efficient computational times on large optimization instances. However, the directed graphs supporting the optimization are often arbitrarily built, defining links between airports. Building a

model that can help manage traffic is of significant interest.

Contrary to most of the approaches previously cited, the present work is data-based and supported by previous research on trajectory clustering into flows [10, 31]. In many en-route Traffic Flow Management tools, the initial position of the aircraft (known with or without uncertainty) is the most important information. A global approach, using tracks and flows features (e.g. routes, flight plans, inter-arrival distances between aircraft) benefits mid-term and long-term en-route air traffic management. Flows provide more predictable and robust estimates than watching aircraft individually [28]. However, limited effort has been put in verifying this claim. As developed in [14, 15], one such way air traffic controllers abstract sectors is according to dominant flow patterns and traffic flow intractions. Many flow characteristics are listed in [35] to describe flow patterns, such as the number of flows, the major flows and their size, the number of crossing flows, etc. Such criteria are a means of estimating and predicting sector demand based on the traffic flow pattern, and of studying the impact of severe weather, as described in [36]. The list of flow characteristics proposed in [35] can also form a basis for the notion of traffic complexity. Nevertheless, more information may be needed for traffic flow managers, in particular the locations of high complexity regions [31]. Estimating air traffic complexity, and its application to determine airspace capacity for dynamic en-route TFM could provide more accurate measures of the state of an airspace than the MAP values.

There is a real need for traffic models to best represent the airspace, in particular the variability and complexity of traffic. In many research approaches for TFM [2], a graph network is formed linking chosen airports. Often times, the network includes the entries and exits of each sector along the way. The resulting network is used to formulate TFM optimization problem. Yet, modeling traffic as if aircraft were

simply traveling along a limited set of predefined air routes and jet routes from an origin to a destination is unrealistic. Figure 2 represents the air routes and jet routes in the Cleveland center overlaid with a density plot depicting the spatial distribution for a day of traffic. It demonstrates traffic is far more diverse than what the routes alone suggest. The en-route TFM problem is sensitive to possible changes in airspace capacity. Obtaining a more precise understanding of the airspace and its capacity is a means of improving the support for TFM under nominal conditions, but also in the presence of perturbations. Data-mining techniques are useful to identify and interpret the behavior of a system. Extracting knowledge from large data sets while making little assumptions enables researchers to build more precise models.

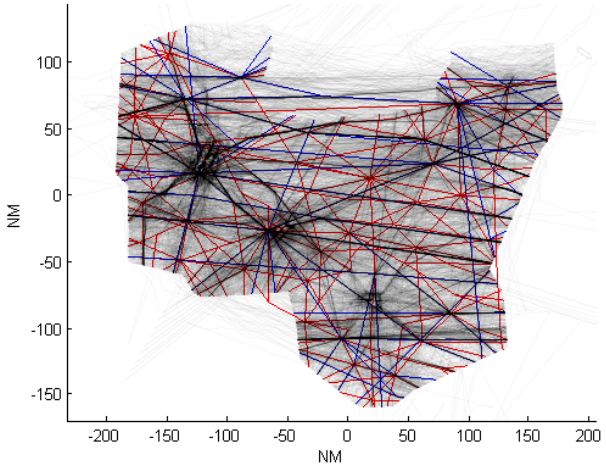


**Figure 1:** Results of the first and second iteration for each commodity, superposed for each.

In the previous research that served as a basis for this thesis [10,31], ETMS data of the Cleveland Center was used to obtain trajectories of aircraft. Cleveland Center was selected because of its significance to the NAS, and because it is considered 'one of the most congested and delay-prone Centers in the Continental United States' [13]. Time-varying flow characteristics, such as geometrical configuration, speed, and probability density function of aircraft spatial distribution within each flow, were determined

using the same data. These flows constitute a detailed model of the airspace.

## *1.2 Objectives of the thesis*

The objective of this thesis is to develop a new way of analyzing and modeling a given airspace from data, under nominal and perturbed conditions. The objective of the thesis will be fulfilled by answering the following research questions :

- Research Question 1: How can data-mining techniques help us develop a methodology for representing an airspace?
- Research Question 2: How can we simulate realistic traffic in an airspace under nominal conditions?
- Research Question 3: How can we make optimal use of the airspace given weather perturbations?

## *1.3 Contributions*

The main contribution of this thesis is to show the use of data-mining techniques in modeling air traffic and calibrating traffic flow management models. This was supported by the following contributions:

- Elaboration of a methodology to build airspace representations as 3D network flow models based on ETMS data.
- Simulation of en-route air traffic using linear optimization and findings from complexity measures.
- Analysis and Simulation of Airspace Degradation and its impact on Air Traffic.

## *1.4 Thesis outline*

This thesis is organized in five chapters. The first chapter has provided an introduction to the work achieved and the motivation behind it. The following chapters address the different research questions asked above.

Chapter 2 concisely presents the previous modeling efforts, from ETMS data to flows [31] that were the support for this thesis.

Chapter 3 addresses Research Question 1. The methodology for abstracting data into a network flow model is developed, where each step is based on data-mining techniques. The validity of rerouting options is discussed, using a $k$-shortest path algorithm.

Chapter 4 addresses Research Question 2. The linear formulation for optimizing Air Traffic using the network flow model built is elaborated. It incorporates new sector constraints, exploiting the flow structure and complexity measures, in order to ensure acceptable controller taskloads. Simulations to validate the importance of the sector constraints and traffic patterns are analyzed.

Chapter 5 addresses Research Question 3. Weather polygons [29] are used to simulate two perturbation scenarios, that occurred during the same period as the ETMS data used to compute the flows. Different simulations are run, aiming at measuring the impact of airspace degradation and validating the model. The results are compared with the ETMS data and discussed.

Chapter 6 draws the conclusions of the thesis and suggests future research perspectives.

# CHAPTER II

# PREVIOUS WORK: CLUSTERING OF TRAJECTORIES INTO FLOWS

This section presents the work done by Gariel et al. [11], that was the basis for this thesis.

The data used to construct the airspace model is taken from Enhanced Traffic Management System (ETMS). Cleveland center is selected because of its significance to the NAS, and because it is considered one of the most congested and delay-prone Centers in the Continental United States [13]. The data includes aircraft trajectories, spatially sampled (longitude, latitude, altitude) every minute. During the 123 days (May to August 2005) covered by the data, all 526,840 aircraft trajectories with at least one point over FL250 are considered, which gives us a subset of data covering the majority of en-route aircraft. After filtering inconsistencies in altitudes, a 'clean' data-set of 338,060 trajectories remains. Figure 2 represents the air routes and jet routes in the Cleveland center overlaid with a density plot depicting the spatial distribution for a day of traffic. It demonstrates traffic is far more diverse than what the routes alone suggest.

The trajectory Clustering Algorithm is defined by the following steps, according to [31]:

1. Remove inconsistencies and format the trajectories.

2. Augment dimensionality of the data by adding features such as heading, polar coordinates, etc.

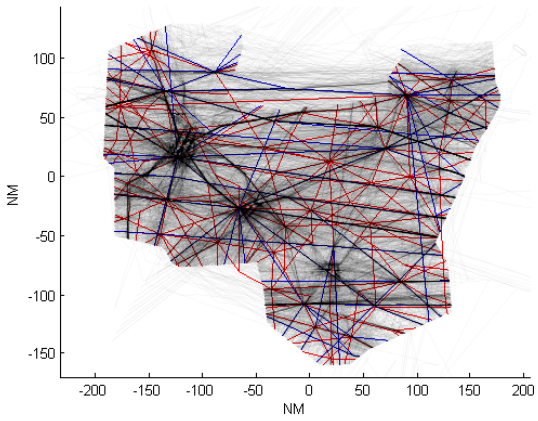


**Figure 2:** Density Plot of one day of traffic against the air routes of the NAS

3. Apply hierarchical clustering. Organize and divide the trajectories by altitude and attitude to create separate data sets.

4. Normalize each feature and concatenate the data into a single row vector for each flight. Each column corresponds to a feature.

5. Apply a Principal Component Analysis (PCA) on the matrices, and reduce the dimensionality of the data by keeping only some principal components.

6. Cluster the values of the projections using a density-based clustering algorithm (DBSCAN).

7. Obtain clusters of trajectories and outliers for each altitude and attitude category.

Figure 3 shows an ascending flow obtained by the above clustering algorithm.

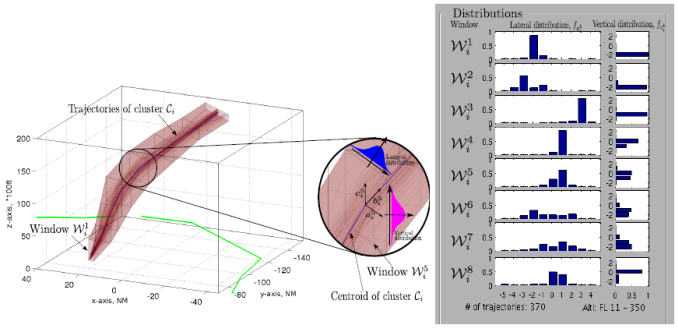


**Figure 3:** A 3D representation of an ascending flow with the geometric distributions of trajectories.

Following categorization and clustering, about 80% of the trajectories are grouped into 690 clusters, or flows, and the remaining 20% are outliers (modeled separately). The outliers are trajectories that do not exhibit the same features as most other trajectories. Figure 4 presents a 2D and a 3D view of the centroids of all clusters. Blue lines represent westbound traffic, yellow eastbound, green descending, red ascending. The major airports of Cleveland Center - Cleveland Hopkins airport (CLE), Detroit Metropolitan Wayne County Airport (DTW) and Pittsburgh International Airport (PIT) - are clearly identifiable by the clusters corresponding to ascending and descending traffic. The fraction of outliers is relatively constant throughout the day. The results obtained demonstrate that the clustering remains consistent over a broad range of parameterizations (time of day, altitude/attitude). Therefore, clustering yields a model that can be utilized for subsequent complexity analysis.

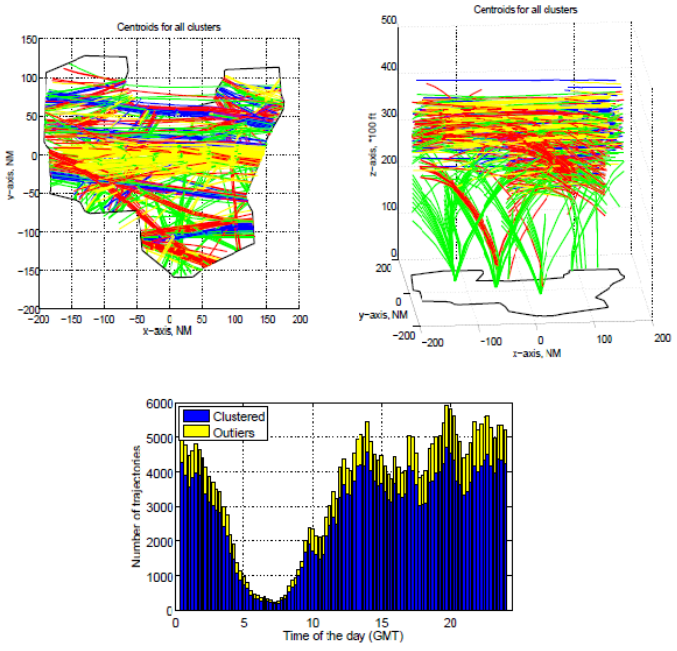


**Figure 4:** Centroids for all traffic flow clusters and outliers distribution.

# CHAPTER III

# TRAFFIC FLOW MANAGEMENT FRAMEWORK

## *3.1 Network building*

The goal of this section is to present a new framework for the en-route TFM problem, that consists in a traffic flow network enabling aircraft to follow a given route or be re-routed if necessary. The support for building this network are the flows created from historical data. A network is a system of nodes and edges linking the nodes. The edges represent the flow corridors in which aircraft fly and the nodes the areas where aircraft enter, change of, or leave a flow. To generate the network, the following steps were carried out.

- The first step is to locate the regions where aircraft can leave a flow and join another. These airspace regions constitute some of the nodes of the future network.
- The second step is to identify the other nodes, which are the spatial areas from which aircraft enter or leave the airspace, whether on the boundaries of the center, or at airports located in the center.
- The third step is to create the edges that link the nodes of the network, to re-create the possible flow routes an aircraft can travel on.

Our interest lies in simulating traffic through the network. Therefore the pairs of entry nodes - exit nodes in the network corresponding to origin-destination pairs are collected in the fourth step, i.e. which nodes aircraft leave and which are the associated nodes aircraft aim at reaching. This corresponds to the demand that is intrinsic to the airspace of the Cleveland center.

### 3.1.1 Identify interactions between flows

The areas where flows spatially interact correspond to areas that engender a high probability of conflict. Such areas include intersections of flows and flow merging. Some of these areas are such that an aircraft may leave the flow it was traveling on and join another.

Two flows have the potential to conflict and interact, if the horizontal distance between their respective centroids is less than 10 NM and the vertical distance to 1000 ft (inside the same flight level). Figure 5 shows two intersecting flows, whereas Figure 6 shows two non-intersecting flows. The midpoint of the segment linking the two closest points on each centroid is defined as the location of the geometric intersection between the two flows. Computing all the geometric intersections between the 690 flows identified by the clustering algorithm yields 16,151 conflict areas located in Cleveland center.

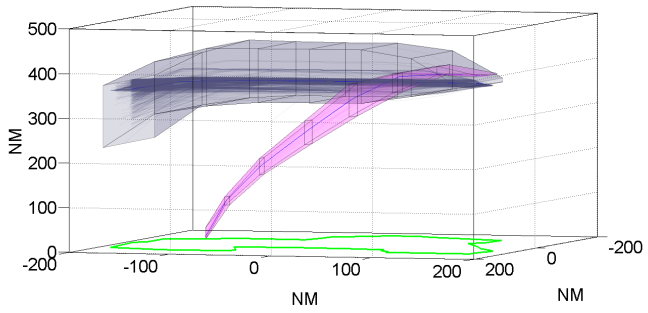


**Figure 5:** Two intersecting flows.

However, our goal is to build the network of all possible routes for an aircraft to fly. Even if there exists a conflict area between two flows, aircraft are not necessarily able to modify their trajectory to fly from one flow to another flow. The possibility of re-routing depends on the geometry of the interaction area of the flows. For instance, an aircraft flying on an ascending route that encounters a descending route, would not and is physically incapable of maneuvering to join the descending one. Therefore

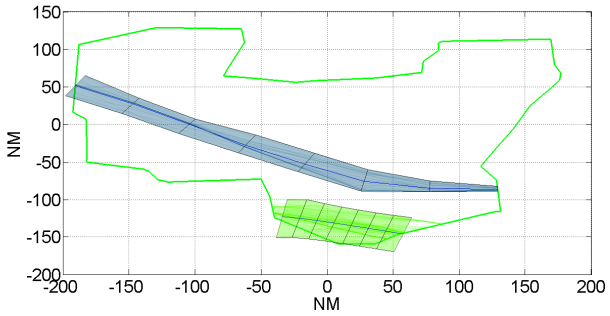


**Figure 6:** Two flows that do not intersect.

a distinction is made between the conflict areas that can support rerouting, and those that cannot. The conflict areas suitable for re-routing are designated as the nodes or vertices of the future network, whereas the remaining conflict areas are called crossings. A conflict area supports re-routing if:

- It is a conflict area between two flows whose phases (i.e. ascending, descending, level) match.

- The angle between the two centroids in this area is less than 30 degrees. This is to ensure that an aircraft is able to maneuver from one flow to another.

- The conflict area is not located within 30 NM of the entry or exit of the flows in the center.

A conflict area satisfying these properties is defined as a node of the network. According to the clustered air traffic flow model, 1188 nodes and 14953 crossings are identified over the Cleveland center, as illustrated in Figures 7 and 8. The crossings do not induce a node in the network, they do not intervene in its construction, for it is meant to be a network of available routes for aircraft. Nevertheless, we store them to use them later as meaningful indicators of the complexity of the airspace.

### 3.1.2 Cluster the network entrances and exits

All flows have an entry and an exit. For en-route flows, the entrances and exits are located at the boundary of the center. For arriving or departing flows, the entrances

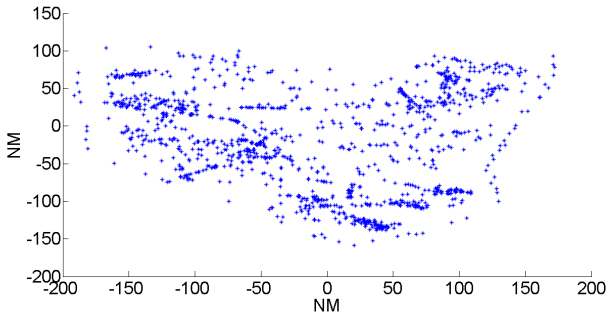


**Figure 7:** Spatial distribution of all nodes from intersections in the center.

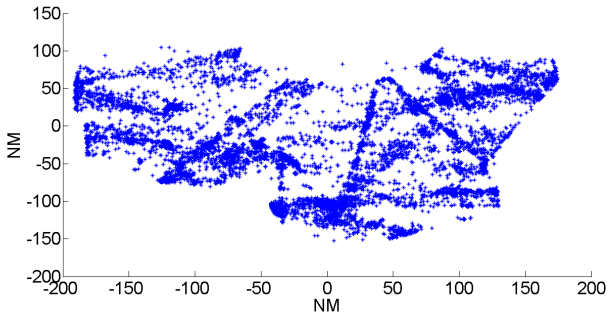


**Figure 8:** Spatial distribution of all crossings in the center.

and exits are at the zero altitude within the center. Observing the distribution of the entrances and exits of the flows in 3D allows us to group them into shared entries and exits.

To determine which entrances or exits are grouped together, a clustering algorithm is applied for each. The distinction between entries and exits prevents aircraft leaving the center through one flow from encountering aircraft entering the center through the same node in the opposite direction. The $k$-means clustering algorithm is chosen because it is simple to execute and adjust. The algorithm clusters the 3D points into $k$ groups, where $k$ is an input parameter, and assigns each point to clusters depending on the distance to the centroid of each cluster. The cluster's centroid is then recomputed and the process begins again. A concern with the clustering is that its assessment of whether the result is good or not is subjective. One usual drawback

of running the k-means algorithm on a 3D dataset is that it prioritizes the x, y-axes over the z-axis because of their relative scale. Thus, to overcome this problem, the implementation of $k$-means was calibrated by running it for different values of $k$ and various relative weighting of the z-axis versus the x, y axes.

The values of $k$ were selected to be 40 and 50 for the entrances and exits, respectively, and by dividing the altitude by a factor of 10. These values are different for the entrances and exits because the spatial distribution of the entry points and exit points of the flows is not the same. The resulting clusters define additional nodes in the network. Their distribution in the center is displayed below, in Figures 9 and 10 for the entry nodes and exit nodes.

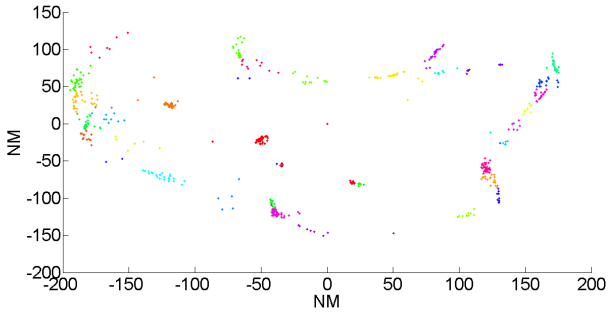


**Figure 9:** Results of k-means clustering on the entry points.

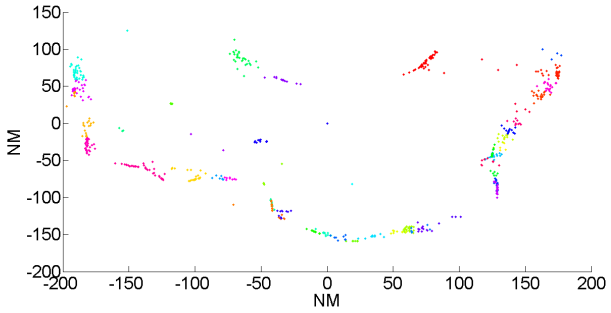


**Figure 10:** Results of k-means clustering on the exit points.

In its complete form, including entry, exit and intersections, the network contains 1288 nodes, 1188 of which represent conflict areas suitable for rerouting.

### 3.1.3 Build the edges of the network

The nodes of the network are then linked together with edges in a suitable manner, representative of the previously described traffic flow model. On each flow, an edge is defined between all pairs of consecutive nodes (whether entry, intersection enabling rerouting, exit) along the flow. Any redundant edges, i.e. those edges corresponding to two flows, but linking the same nodes, are removed. For example, in Figures 11 and 12, there are six flows, whose entries are all clustered together, and whose exits are clustered into two distinct clusters. In the center, there are four conflict areas suitable for rerouting between different pairs of flows, labeled by the red triangles. Edges connect nodes representing the conflict areas suitable for rerouting along the flow, starting with an entry node and ending with an exit node. Redundant edges at entrances or exits are eliminated. For instance, there is only one edge, $Edge_3$, between $N_4$ and $N_6$ in Figure 12, that corresponds to the end of flows $F_2$ and $F_5$.

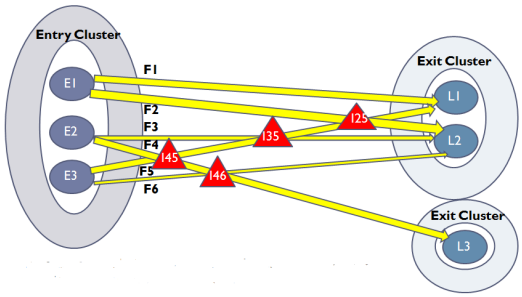


**Figure 11:** Simple example of flow interactions.

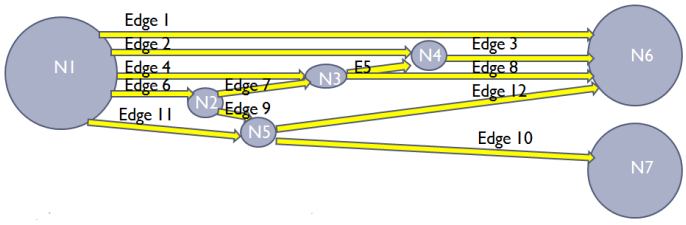


**Figure 12:** Create the edges between the nodes.

### 3.1.4 Collect Origin-Destination Pairs and Historical Traffic Pattern

By simply exploiting the data contained in the flows, the entry and exit nodes of the network have been created, as well as the edges linking the nodes. Our interest lies in simulating traffic as realistically as possible, that is, simulating traffic flying from its origin in the center to its destination, as shown by historical data. In order to do this, the origin-destination pair for each flow is stored, using the entry and exit data gathered by the $k$-means clustering in the previous sub-section. Hence the 218 origin-destination node pairs of the present network are obtained. A commodity is defined as all aircraft having the same origin-destination nodes pair.

The number of trajectories clustered in each flow provides the relative importance of each flow with regard to the total traffic. This process is extended to the origin-destination pairs, or commodities, to determine the relative importance of each commodity in regard to the total traffic. The fraction of the total traffic historically associated with each commodity is denoted as $f_k$, for $k$ between 1 and 218. Thus the main routes traveled in the center are identified, as illustrated in Figure 13. For instance, 50% of the traffic is historically associated with 18 commodities, that is 8% only of the commodities, while 90% of traffic is traveling on 88 commodities, i.e. 40% of the commodities.

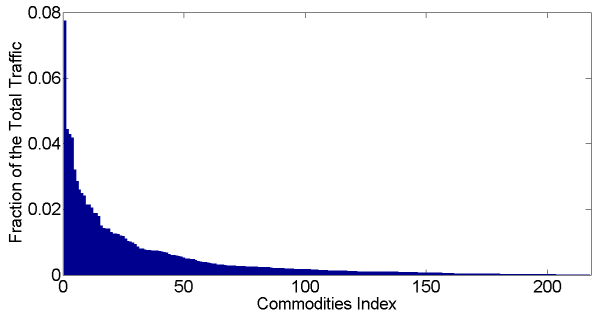


**Figure 13:** Relative fraction of traffic for each OD pair.

## *3.2 Paths in the graph*

Having built a network of rerouting options, determining which routes an aircraft may fly when entering the airspace is of significant interest. In this subsection, we examine the shortest routes for an aircraft to travel on between its origin and its destination in the given airspace center, in order to gain more insight on the paths available.

The shortest routes between the origin and destination nodes of each of the 218 pairs are computed using a $k$-shortest path algorithm, based on Djikstra's algorithm in a graph. The algorithm is applied to the graph constructed above, which is considered as a weighted graph, where the weights correspond to the euclidean distance of the edges. For simplicity, these weights are computed as the exact length between the nodes of an edge, and not as the actual length of the centroid from which the edge was built, converting the nautical miles and flight levels into feet. For computational reasons, the parameter $k$ was set to 5, believing that this should provide a large enough number of alternative routes. The computations involve trying to find $k$ routes for 218 pairs of nodes, in a graph comprising 1288 nodes.

First, 81% of origin-destination pairs have five routes available, where these routes may have common edges. Only 19% of origin-destination pairs have fewer than five routes, and about 9% have only a single route available. The average number of routes per origin-destination pairs is 4.4 out of 5. Besides, to evaluate how different the routes available for a given origin-destination pair are, the length of the longest path, or the k-th path, is compared with the length of the shortest path. The results show that on average, the longest path is about 6% longer than the shortest path, and only about 10% of the origin-destination pairs have a longest path exceeding the

shortest by more than 15%. This suggests that most of the routes found can be considered close to equivalent in term of length. A complicated question is to understand how different or close they may be, in the sense that having similar length does not imply that they are the same, or follow the same edges or nodes. From Figures 14 and 15, it is clear that some paths share common portions, whereas others do not.

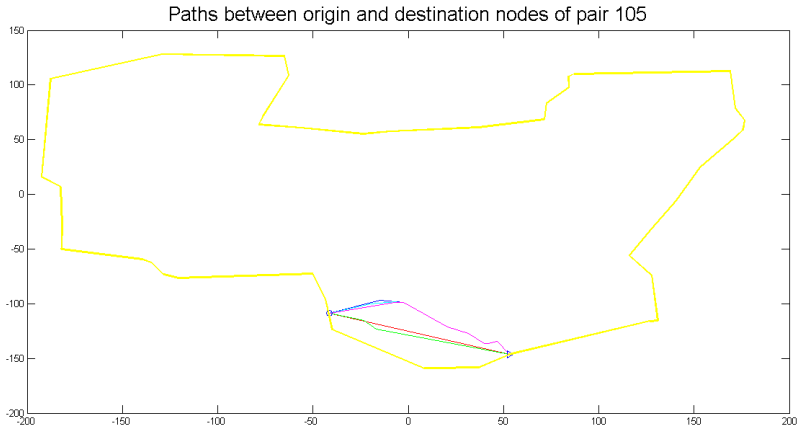


**Figure 14:** Five shortest paths between the origin and destination node of pair 105.

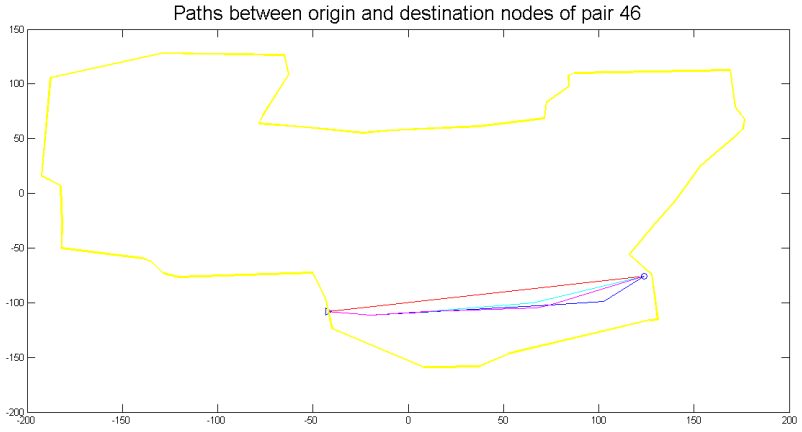


**Figure 15:** Five shortest paths between the origin and destination node of pair 46.

Also, the actual length of a path gives little indication on how complex it is, meaning, how many nodes it goes through for instance. For a given origin-destination pair,

the maximum number of nodes in a path is between 2 and 22 nodes, and is on average of about 8 nodes. A path may go through more nodes than another and still be of about the same length if the edges in between are short. This happens especially in the most intricate regions of the airspace, where several flows have conflict areas with many others.

The network developed is exhaustive, in the sense that it is built on all the trajectories observed during more than a hundred days. It is likely that only some subset of the network is used at a given time of a day. It is also likely that some parts of the network play a more important role in the airspace than others. For this reason, among all the paths found between pairs, the overall occurrence of each node in a path was computed. Out of the 960 paths computed for all the origin-destination pairs, a node appeared on average in 5 paths. Yet, about 25% of the nodes had a zero occurrence, meaning they did not belong to any of the shortest paths. About 15% of the nodes occurred more than 10 times, which suggests that these particular nodes may be more crucial to the network than others.

This graph analysis of the network through the shortest paths highlights some of its characteristics, yet it only addresses the notion of best (shortest) route for an aircraft to fly on. The end of the next section will provide more insight on what a best route might be.

# CHAPTER IV

# AIR TRAFFIC OPTIMIZATION

## *4.1 Linear optimization model*

The network model is intended to provide support for further analysis of the airspace. In the present section, different means of addressing en-route traffic flow management optimization problems are discussed, using the previous network and linear formulations. A set of common constraints for various en-route Traffic Flow Management problems are defined, thereby providing a framework to modify the objective function $H$ and provide additional constraints as necessary. Next, a non-standard set of constraints is added, to account for sector capacity as a result of controller workload. These constraints are an alternative to MAP values traditionally used. The flow and sector constraints are described in the proceeding subsections. The general problem is of the following form :

$$\begin{aligned} &\text{maximize H} \\ &\text{subject to :} \\ &\qquad flow \quad constraints \\ &\qquad sector \quad constraints \end{aligned} \tag{1}$$

## *4.2 Flow constraints*

To solve the Traffic Flow Management Problem in terms of flow rates still requires that aircraft respect separation distances while traversing the airspace on each edge. This is accomplished by constraining the number of aircraft allowed on each edge during a given time period. Aircraft are assumed to travel at a uniform speed between

origin and destination. Define the variable $x_i$ to be the flow rate on the edge $i \in \mathbf{E}$, where $\mathbf{E}$ is the set of edges of the network, numbered, $[1 : 3085]$, and $\delta$ being 20 minutes. The following condition must hold

$$\forall i \in \mathbf{E}, x_i \leq r_{max}, \tag{2}$$

where $r_{max} = \frac{s*\delta}{d_{min}}$, $s = 8.7NM/min$ is the average speed of an aircraft and $d_{min} = 5NM$ is the minimum separation between aircraft. It is assumed that all aircraft travel at the same speed at any altitude, and that aircraft queue on each edge.

Commodities compete to occupy edges, hence the need to track the distribution of commodities on each edge as well as the total traffic. Denoting $y_k^i$ then flow rate of commodity $k$ on edge $i$, $i \in \mathbf{E}$, $k \in \mathbf{C}$, where $\mathbf{C}$ is the set of commodities, numbered, $[1 : 218]$. The following condition ensures that commodities share the flow rate allowed on each edge

$$\forall i \in \mathbf{E}, x_i = \sum_{k \in \mathbf{C}} y_k^i. \tag{3}$$

In order to compare the demand for each commodity, the total flow rate corresponding to each commodity entering the center, or equivalently, leaving the center, is computed. Denoting $s_k$ the demand for the commodity $k$, $k \in \mathbf{C}$, and $\mathbf{E^k_{entry}}$, the set of edges leaving the origin node of the $k^{th}$ commodity, and $\mathbf{E^k_{exit}}$, the set of edges arriving at the destination node of the $k^{th}$ commodity / origin destination pair, the following conditions are required

$$\forall k \in \mathbf{C}, s_k = \sum_{i \in \mathbf{E^k_{entry}}} y_k^i, \tag{4}$$

$$\forall k \in \mathbf{C}, s_k = \sum_{i \in \mathbf{E^k_{exit}}} y_k^i. \tag{5}$$

At each node corresponding to an intersection supporting rerouting ( i.e. all nodes except the entry and exit nodes), flow conservation is enforced. Each intersection node

has two arriving edges, $i$ and $j$, and two departing edges, $l$ and $m$. More precisely, the total flow rate on the edges, as well as the flow rate for each commodity traveling on the edges, are conserved, by the constraints below:

$$x_i + x_j = x_l + x_m \tag{6}$$

$$\forall k \in \mathbf{C}, y_k^i + y_k^j = y_k^l + y_k^m. \tag{7}$$

To ensure that all aircraft entering the center leave the center, a global flow conservation constraint is required. The following constraints are enforced on two sets of edges, $\mathbf{E_{entry}}$ , the set of all edges leaving entry nodes, and $\mathbf{E_{exit}}$, the set of all edges arriving on exit nodes.

$$\sum_{i \in \mathbf{E_{entry}}} x_i = \sum_{j \in \mathbf{E_{exit}}} x_j. \tag{8}$$

This formulation that considers all constraints from (2) to (8) results, results in an unsimplified linear program of approximately 273,000 lines. This set of constraints is denoted as "flow constraints".

## *4.3 Sector constraints*

The ideas in this section are taken from Vela et al. [1, 38] and expanded upon as follows.

The projected growth in air traffic demand over the next twenty years is likely to generate traffic that will test the control capacity of air traffic controllers. Both the FAA, and EUROCONTROL, recognize the need to predict air traffic demands for en route sectors, and plan for staffing requirements for tactical controller positions. Consequently, there has been significant investment in the development of workload metrics to evaluate when and where capacity issues may lead to safety concerns. Thus, in addition to a traffic model described previously, a model representing the actions and responses of human air traffic controllers is presented.

The work in this section seeks an appropriate estimate of when controller overload occurs. That is, a means of determining when controllers encounter traffic scenarios that are beyond their capabilities. The process described here in detecting unmanageable traffic levels is based on a taskload and communications model that is associated with the control process between air traffic controllers and aircraft.

### 4.3.1 Controller taskload

Controller workload is defined by Stein as "the amount of effort, both physical and psychological, expended in response to system demands (task load) and also in accordance with the operators internal standard of performance [37]." As it stands, the capacity to properly manage and separate air traffic directly depends on the controller workload [4]. Unfortunately, controller workload is difficult to measure quantitatively and depends on each individual controller's capability and perception. In current operations, instead of relying on controller workload as a measure for sector capacities, the Federal Aviation Administration has relied on a simple proxy: the number of aircraft present in a sector. The limit on this value is established by the Monitor Alert Parameter (MAP). If aircraft counts are within the MAP value, then it is assumed that traffic conditions are within the controller's abilities. However, MAP values do not accurately represent sector capacity - and often times lead to congestion, or conversely, under-utilization of the airspace because they does not accurately address performance limits.

Radio communication time has been considered an objective metric to evaluate controller workload while managing traffic. A series of experiments has concluded that realistic radio activities can be used to provide objective measures of workload [5, 8, 34]. Additionally, other studies have demonstrated the high correlation between communication duration and controller workload, thereby effectively validating communication time as another workload measure [20, 27]. By its very nature,

communication time can be related to bandwidth limitations within the human-in-the-loop control system. While a detailed analysis of the different type of communication events provided accurate estimates, they also concluded that the total number and duration of communication events were significantly correlated with controller workload.

Because communication is used in both the management and control of aircraft, if events within the airspace require greater amounts of communication than time permits, then some fundamental limit has been reached. Accordingly, this section, and the proposed communication model, studies how communication requirements can exceed reasonable capabilities of the air traffic controller.

In current operations, each aircraft passing through a sector is communicated with at least twice by the managing air traffic controller: once to acknowledge the aircraft as it enters the sector and again when the aircraft is handed-off to the next sector. Another prevalent communication type typically occurs when an airspace is congested and there is the potential for conflict. Provided sufficient concern by air traffic controllers exists that a pair of aircraft might conflict, then a resolution command is issued. In the case of a potential conflict, air traffic controllers must determine safe routes for all aircraft and communicate them to each pilot. For this process to occur in a safe manner, there must also be sufficient time for the controller to gain situational awareness and to monitor conformance of the resolution commands. Finally (as part of the current system of clearance based control, in which requests are made by pilots, and verified for safety by the controller), any request for changes in heading, speed or altitude requires communication. The most common of these pilot requests is for altitude changes, either to ascend or descend in flight-level. Accordingly, the workload model considers common tasks, and estimates the amount of time-effort the controller must spend on each. The tasks include:

- aircraft acknowledgements,

- altitude clearances,
- hand-offs,
- monitoring turning aircraft,
- resolving potential conflicts.

Based on a weighted sum of the number of events associated with each task, a running cost associated with airspace management tasks is calculated. The workload model formulated is consistent with the network formulation, the proposed workload measure can be calculated according to the flow rates, $x_i$, throughout the center.

We believe that a model that considers event rates across each sector, and limits an expected workload estimate, is potentially more relevant than constraining aircraft counts. As traffic routes become increasingly disrupted, the standards by which MAP values are generated no longer apply. The re-routing of traffic produces spatial aircraft distributions that can either simplify or complicate traffic management. By accounting for potential conflicts a more meaningful measure is introduced. Indeed, the conflict-detection and resolution process can be quite taxing on the controller. For just, identifying and resolving a potential conflict, one study estimates that controllers spend up to 27 seconds on the task [7].

For an arbitrary sector $S$, the communications taskload is given by summing the weighted effort required for the six tasks listed above (acknowledgements, clearances, turning aircraft, etc.). The associated equation is

$$\sum_{i=1}^{5} C_i^S R_i^S. \tag{9}$$

In (9), the value $R_i^S$ represents the expected rate associated with the $i^{th}$ task inside of sector $S$. The weighting $C_i^S$ is the average amount of time spent on the corresponding task. Accordingly, the total sum is the total amount of time effort expected by the air traffic controller for a given period of time. To maintain reasonable workload the

total sum should be bounded according to the performance capabilities of air traffic controllers. Normalizing all the weightings and rates, the final sum can represent the percent of time spent performing the required tasks.

### 4.3.2 Tasks performed by the controller

The process by which each event rate, $R_i^S$, occurs is detailed in the following subsections. In order, each rate, $R_i^S$, corresponds to: acknowledgments; hand-offs; altitude clearances; monitoring turning aircraft; identifying and monitoring potential conflict situations; and resolving potential conflicts.

**Acknowledgments, Hand-offs, and Altitude Clearances** The first two event rates, $R_1^S$ and $R_2^S$, correspond to routine communications between pilots and controllers: acknowledgments and hand-offs at sector boundaries. At a minimum, each aircraft is communicated with at least twice by the managing air traffic controller, once to acknowledge the aircraft as it enters the sector, and again when the aircraft leaves as part of the hand-off to the next sector.

Flows entering or exiting a sector are divided into the sets $In(S)$ and $Out(S)$. Denoting $x_i$ to be the rate of aircraft in or out of a sector along a particular flow, the rates $R_1^S$ and $R_2^S$ are given by

$$R_1^S = \sum_{i \in In(S)} x_i, \tag{10}$$

and

$$R_2^S = \sum_{i \in Out(S)} x_i. \tag{11}$$

The event process for altitude clearances are handled in a similar manner. Those entry flows that are associated with ascending or descending traffic flows are included in the set $Alt(S)$. The rate of events associated with altitude clearances are given by

$$R_3^S = \sum_{i \in Alt(S)} x_i. \tag{12}$$

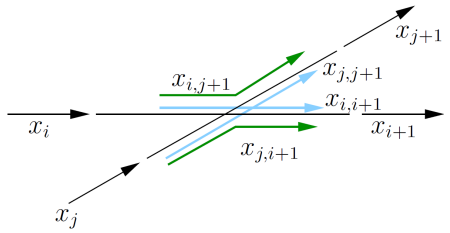


**Figure 16:** Intersection between edges in the network.

When calculating the total time-effort associated with each event process, i.e. $C_i^S R_i^S$, care must be taken not to double-count events. In particular, ascending and descending edges entering a sector must only be accounted for once. As such, while $C_1^S$ accounts for any nominal time spent acknowledging an aircraft entering the sector $S$, $C_3^S$ accounts for the additional time spent processing a request to issue an altitude clearance to the entering aircraft

**Turning Aircraft** Turning aircraft was identified by researchers as a relevant factor in estimating controller workload. In the case of disruptions, the relevance of turning aircraft becomes greater as a larger fraction of aircraft may require rerouting. In regards to the model formulation, a turn occurs at an intersection when traffic is diverted from one flow to another.

Consider an arbitrary intersection, as illustrated in Figure 16. The traffic along each entering edge has the option to continue along the same path, or to be rerouted. For the traffic flow $i$, the incoming traffic rate $x_i$ is divided between $x_{i,i+1}$ and $x_{i,j+1}$, corresponding to the outbound rates for continuing onwards or rerouting. Accordingly, conservation laws require the constraint equations at any intersection between edges $i$ and $j$, that exit along edges $i+1$ and $j+1$. The constraint equations are

given by

$$\begin{aligned} x_i &= x_{i,i+1} + x_{i,j+1} \\ x_{i+1} &= x_{i,i+1} + x_{j,i+1} \\ x_j &= x_{j,j+1} + x_{j,i+1} \\ x_{j+1} &= x_{j,j+1} + x_{i,j+1} \end{aligned} \tag{13}$$

Therefore, at any intersection $k$, the rate of turning aircraft at the intersection, $R^S_{4,I}$ is

$$R^S_{4,k} = x_{i,j+1} + x_{j,i+1}. \tag{14}$$

And the total number rate of turning aircraft at the $K$ intersections within the sector $S$ is

$$R^S_4 = \sum_{k=1\ldots K} R^S_{4,k}. \tag{15}$$

The time-effort cost of turning aircraft, given by $C^S_4 R^S_4$, is a measure of the amount of time controllers take to ensure aircraft conform to their intended path. Additional time must consider any potential conflicts that might occur at the intersection, whether the aircraft are turning or not. This additional effort is considered next.

**Potential conflicts** The potential for conflicts occurs at intersections between flows. A potential conflict is deemed to require effort from the controller when two aircraft come within 9NM miles of each other. Denoting $R^S_5$ to be the event rate for potential conflicts that require resolution, for an arbitrary level intersection $k$, such as the one illustrated in Figure 16, the expected rate of potential conflicts is given by

$$R^{conflict} = x_i x_j DV, \tag{16}$$

where, $x_i$ and $x_j$ are the arrival rates into the intersection, and $V$ is the expected groundspeed of aircraft [32]. The value $D$ represents a distance interval during which aircraft along each flow can interact; the distance is calculated by the equation

$$D = \frac{2AV\sqrt{2(1-\cos\theta)}}{V\sin\theta}. \tag{17}$$

The value $A$ in (17) represents the separation distance or minimum miss-distance between aircraft indicating if aircraft are issued resolution commands or not. When $A = 9$NM, then each $R^S_{5,k}$ represents the event rate for how often aircraft come within 9NM of each other and are maneuvered.

In the current form, (17) is a nonlinear equation that cannot be handled by standard linear optimization algorithms. As such, the equation is approximated using a Taylor Series approximation. Denoting $\hat{x}_i$ to be the estimated traffic flow rate along an edge $i$, the Taylor approximation of (17), and the estimated rate of potential conflicts is calculated by the equation

$$R^S_{5,k} = \hat{x}_i \hat{x}_j DV + (x_i - \hat{x}_i)\hat{x}_j DV + (x_j - \hat{x}_j)\hat{x}_i DV. \tag{18}$$

Much like the cases acknowledgments, hand-off clearances, the weighting values for conflict-event process should be selected accordingly. For potential conflict coming within 9NM the weighting value is selected to be $C^S_5 = 30$ seconds.

While not detailed here, (18) is also applied to merge points and turning aircraft. In both these cases, there is the potential for conflicts, and the event rate can be approximate by the same equation. Additionally, while not an exact solution, crossings and intersections of mixed ascending, descending, and level edges make use of (18) to approximate the conflict event rate.

Taking into account some factors introduced by dynamic density and controller-pilot communication times, the communication and bandwidth model is used to approximate constraints on the expected workload a controller should be exposed to. The workload model considers common tasks, and estimates the amount of time-effort the controller must spend on each. The tasks include:

- acknowledgments,
- altitude clearances,
- hand-offs,

- monitoring turning aircraft,
- resolving potential conflicts.

Based on a weighted sum of the number of events associated with each task, a running cost associated with airspace management tasks is calculated. The workload model formulated is consistent with the network formulation, the proposed workload measure can be calculated according to the flow rates, $x_i$, throughout the center.

For an arbitrary sector $S$, the workload constraint is given by summing the weighted effort required for the six tasks listed above (acknowledgments, clearances, turning aircraft, etc.). The associated equation is

$$\sum_{i=1}^{5} C_i^S R_i^S \leq \bar{W}^S, \tag{19}$$

where $\bar{W}^S$ is a measure of the maximum allowed workload. In (19), the value $R_i^S$ represents the expected rate associated with the $i^{th}$ task inside of sector $S$. The weighting $C_i^S$ is the average amount of time spent on the corresponding task. Accordingly, the total sum is the total amount of time effort expected by the air traffic controller for a given period of time. To maintain reasonable workload, the bound on the constraint, i.e. $\bar{W}^S$, should be selected carefully. Normalizing all the weightings and rates, the value $\bar{W}^S$ represents the upper-bound on the percent of time spent performing the required tasks. In simulations, the value $\bar{W}^S = .5$ is selected.

### 4.3.3 Sector constraints review

By estimating the expected rate of acknowledgments, hand-offs, clearances, turning aircraft, and potential conflicts requiring resolutions, a controller taskload model is generated. Each event process for a sector $S$, is associated with a rate and a cost, $R_i^S$ and $C_i^S$. Summing the weighted costs, a total for the amount of time-effort made by the air traffic controller is estimated. Ideally, the time-effort from the controller

should be within reasonable limits to ensure manageable workloads by the air traffic controller.

We must note, that selection of the values for each $C_i^S$ is left to some debate, and perhaps importantly, so is the workload bound $\bar{W}^S$. However, there must be a recognition that the MAP value used in current day operations are not optimized to consider weather disruptions and re-routing. As such, we believe our proposed model is a suitable alternative to handling dynamic traffic and weather scenarios in which re-routing is ubiquitous.

#### *4.3.3.1 Iterative Implementation*

The inclusion of (17) into a linear program necessitates an iterative process for coming to a final solution. This is because reasonable estimate values for each $\hat{x}_i$ are most likely unknown - especially in the case of significant re-routings. As such, an iterative process for solving the network flow problem in (1) is proposed. The process is described in below.

**Procedure 1** Iterative Implementation

$\hat{x}_i = 0 \forall i$

**while** $||\hat{x} - x|| > \epsilon$ **do**

$\hat{x}* = \arg\min_x maxflow(\hat{x})$

$\hat{x} = x^*$

**end while**

Initially, each $\hat{x}_i$ is set to 0. Setting the estimated traffic flow rates to 0 results in a solution to the Max-Flow problem in (1) that does not consider potential conflicts in the sector workload constraint equations. When all $\hat{x}_i = 0$ then $R_{5,k}^S = 0$ and $R_{6,k}^S = 0$ at each intersection for all sectors. In this manner, the initial cost to the network optimization problem serves as an upper-bound. Using the solution to the Max-Flow problem, the flow rate estimates for each $x_i$ are updated until convergence

occurs.

## *4.4 Simulation results*

All the Traffic Flow Management problems later posed are solved using the CPLEX solver. Because of the sector workload constraints, each simulation is run multiple times, until convergence, according to the iterative implementation stated above. Again the first iteration of solving the TFM problem assumes no conflict, and for each following iteration, the results of the previous simulation are plugged in to refine the solution and take into account the conflicts between aircraft in different flows.

### 4.4.1 Importance of sector constraints

To verify that the sector constraints are indeed the limiting constraints, the following linear problem is solved :

$$\begin{aligned} &\text{maximize } \textstyle\sum_{k \in \mathbf{C}} s_k \\ &\text{subject to :} \\ &\qquad flow\ constraints \end{aligned} \tag{20}$$

This problem aims at maximizing the throughput of the center, which is equivalent to finding the demand, i.e. the maximum number of aircraft that can flow through the center during a given time interval, without the controller workload constraints. This is equivalent to computing the maximum throughput of the center. The objective, i.e. the sum of all demand, is 22,960 aircraft for a 20 minutes interval. In this case, 3020 edges out of 3085 are used. Further, the 3020 edges are fully occupied, meaning that the maximum rate allowed on these edges is reached, according to (20). The demand distribution is represented in Figure 17. This demand distribution shows that, because of the degree of the entry and exit nodes and of the number of available routes between them, some commodities have the potential to accommodate more aircraft than others.

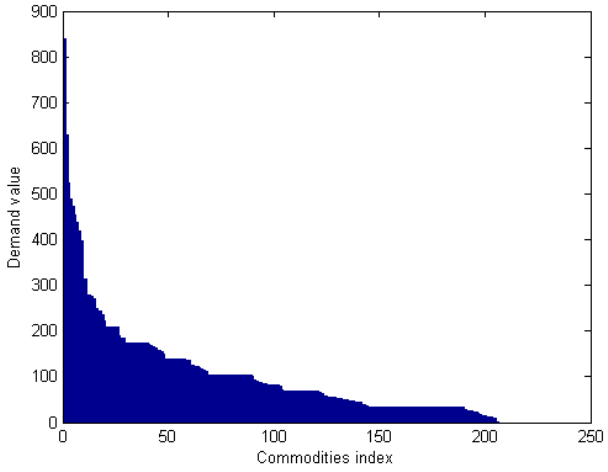


**Figure 17:** Demand distribution when maximizing the demand, without sector constraints.

Secondly, we try and estimate the actual maximum throughput of the center, that is, when taking into account controller workload, as described in the previous subsection. This is formulated as :

$$\begin{aligned} &\text{maximize } \textstyle\sum_{k \in \mathbf{C}} s_k \\ &\text{subject to :} \\ &\qquad flow\ constraints \\ &\qquad sector\ constraints \end{aligned} \tag{21}$$

The demand distribution obtained from (21) is displayed in Figure 18. The objective, i.e. the maximum demand for the center, is 5,576 aircraft for a 20 minutes interval for the first iteration, which decreases to 3,097 for the second iteration due to the limitations introduced by the sector constraints. The objective value of the second iteration is only 14% of the objective obtained when maximizing the throughput without sector constraints. The objective value also decreases by almost 45% from the first to the second iteration, i.e. from a no-conflict scenario to a scenario taking into account the additional workload for the controller caused by conflicts.

While expected, the significant change in center throughput demonstrates that the sector constraints are indeed the limiting factors to maximizing the airspace capacity. Besides, as seen in Figure 18, only 40 commodities out of 218 are traveled in the first iteration, and 41 in the second. The aircraft occupy 518 edges out of 3085 in the first iteration, and 570 in the second. This highlights that if the goal is simply to maximize the throughput, then the commodities with the highest possible flow rates have priority, and the edges generating the minimum number of conflicts are occupied. However, such a traffic pattern is only of interest to define an upper bound on the maximum throughput of a center. It does not reflect the realities of air traffic patterns observed.

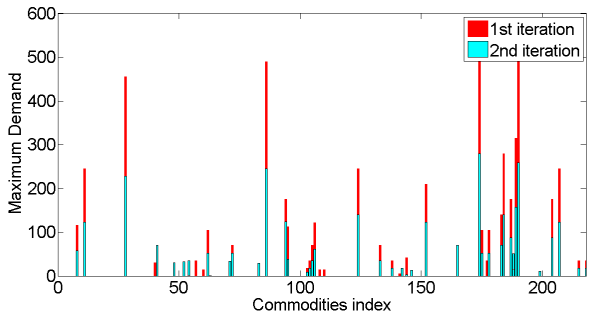


**Figure 18:** Results of the first and second iteration for each commodity, superposed for each, when maximizing the demand.

### 4.4.2 Maximum unimpeded flow for a commodity

This problem considers the maximum unimpeded flow for each of the 218 commodities. Therefore, for all $k \in \mathbf{C}$, (the set of commodities, $[1 : 218]$), the following optimization problem is solved:

$$\begin{aligned} &\text{maximize } s_k \\ &\text{subject to :} \\ &\qquad flow\ constraints \\ &\qquad sector\ constraints \end{aligned} \tag{22}$$

The demand distributions for each of the simulation of (22) are superposed in Figures 19 and 20. The results of each of the 218 optimization problems provide an upper bound on the maximum flow rate for each commodity. This bound is attained only if one commodity is favored. From the first to the second iteration, the bound decreases considerably for each commodity, because possible conflicts between aircraft are taken into account and they modify the measure of controller workload. These results highlight two facts. First, each commodity, if it were the only commodity traveling on the network, would have a greater demand than when competing against other commodities in the network. Second, even if only one commodity is considered, the demand from the second iteration is lower than the first. This demonstrates that conflicts occur between aircraft from the same commodity. Indeed, depending on the geometry of the network, a few or many routes are available for all aircraft of a commodity. If only one commodity is considered, all available routes are taken by aircraft associated with the commodity, while respecting sector constraints. As such, two aircraft with the same entry node and exit node in the center can take different routes, which may interact, hence generating conflicts. It should be noted that the formulation above does not consider preferences associated to cost on the routes.

### 4.4.3 The influence of traffic demand patterns

The previous problems solved were only of theoretical interest. The next problem focuses on historical traffic patterns, as stated in Section 7, Step 4. A new approach is adopted, in which traffic demand patterns are fixed. The distribution of the total

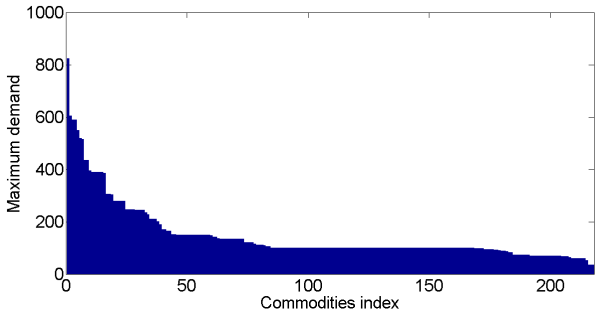


**Figure 19:** Results of the first iteration for each commodity, ordered by descending values.

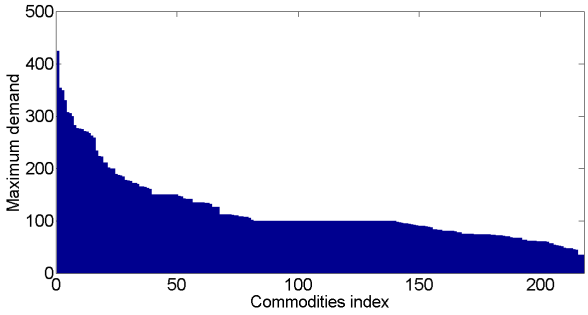


**Figure 20:** Results of the second iteration for each commodity, ordered by descending values.

traffic corresponding to each commodity $k$, $f_k$, using historical data was extracted. Defining a gain $G$ as the total throughput of the center, and forcing the demand for each commodity to fit the distribution of traffic found earlier, another simulation is run. The fixed demand pattern from data is formulated as

$$\begin{aligned} &\text{maximize } G \\ &\text{subject to :} \\ &\qquad \forall k \in \mathbf{C}, s_k = G f_k \qquad (23) \\ &\qquad flow\ constraints \\ &\qquad sector\ constraints \end{aligned}$$

where $f_k$ is the fraction of the total traffic for the commodity $k$, and $\sum_{k \in \mathbf{C}} f_k = 1$.

The edges occupancy distribution obtained from (23) is shown in Figure 21. The demand distribution is fixed, and identical to the one displayed in Figure 13. The first iteration yields $G_{max} = 288$ aircraft for a 20 minutes interval, whereas the third gives $G_{max} = 282$. There are 329 edges out of 3085 occupied in the first iteration, and by the third iteration, 1353 are used. These results show that forcing the traffic to fit demand patterns also forces one to acknowledge controller limitations; traffic almost always generates conflicts. The maximum throughput of the center with a fixed demand pattern is considerably inferior to the maximum throughput in the example from (21). Moreover, forcing the traffic distribution to follow the historical data also forces the aircraft distribution to spread out on the edges.

Several observations can be drawn from these results. First, as indicated by the growth in the number of edges utilized between the 1st and 3rd iteration, maximizing the throughput of the center is not equivalent to maximizing the throughput corresponding to a historical, demand pattern. When maximizing throughput,the objective value of the total demand is 5,576 aircraft during a 20 minutes interval, whereas it becomes roughly 282 aircraft when maximizing the total demand following a traffic distribution, a 95% decrease. Secondly, when taking into account conflicts, i.e. through each iteration of the algorithm, the gain $G_{max}$ remains relatively stable, while the number of edges occupied grows considerably. This points out the fact that, when traffic loads on edges create a high rate of conflicts, there is a need to spread traffic on a greater number of edges, to ensure fewer interactions. Intuitively, using only a few edges that do not interact is useful when maximizing throughput, which was shown when simply maximizing the demand as in (21). However, it is not true anymore when trying to match a demand pattern.

One of the limiting factors when maximizing a given traffic pattern is the geometry of the network. The available capacity for each commodity to fly on is not correlated with the maximum capacity obtained with the historical traffic demand pattern. The maximum throughput is here constrained by the demand pattern. This factor also forces the maximum gain $G_{max}$ to remain stable, but explains the possible spreading on the edges, because some entry nodes with more departing edges are therefore not working at full demand and can disseminate traffic through the network.

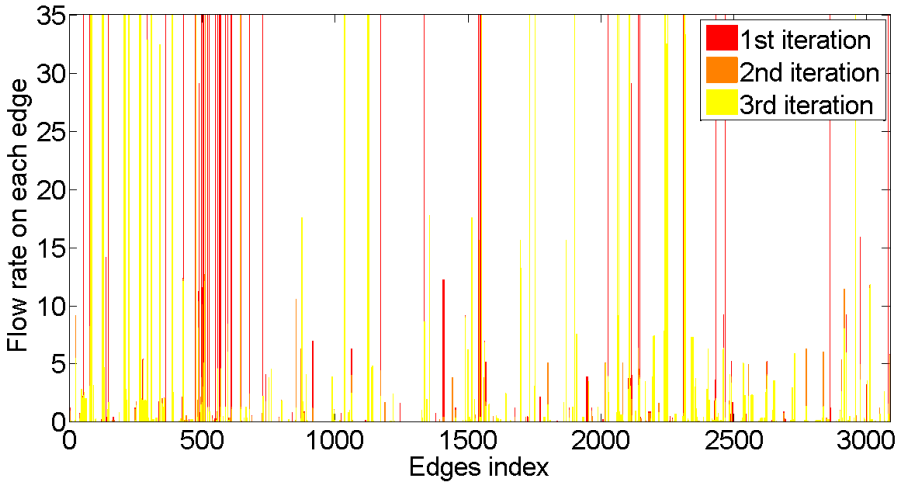


**Figure 21:** Flow rate on each edge, stacked for each iteration.

Since the historical traffic demand pattern was computed as an average over a long period of time, this pattern may not be as fixed as suggested before, and allowing for some freedom in the pattern could influence the throughput. To verify this hypothesis, the following problem was solved. It aims at maximizing the throughput, but the

demand constraints are relaxed from + or - 10%.

$$\begin{aligned} &\text{maximize } G \\ &\text{subject to :} \\ &\qquad \forall k \in \mathbf{C}, s_k <= 1.1 G f_k \\ &\qquad \forall k \in \mathbf{C}, s_k >= 0.9 G f_k \\ &\qquad flow\ constraints \\ &\qquad sector\ constraints \end{aligned} \tag{24}$$

The results of the optimization give a throughput of 320 aircraft for the first iteration and 316 for the second iteration, which corresponds to a 12% increase in throughput compared to the scenario above with a fixed demand pattern. A spreading on the network is also observed, from 314 edges occupied in the first iteration to 587 in the second. However, their respective traffic repartition on the edges is different, as shown in Figure 22. The relaxation of the demand constraint greatly modifies the results. This shows that slight modifications in the relative importance of traffic on the same origin-destination pairs impacts the entire airspace, and not only the paths previously occupied.

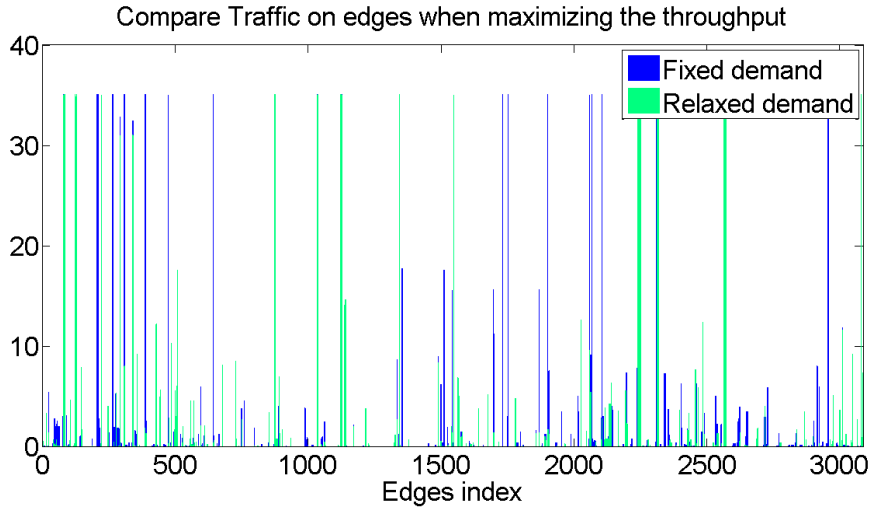


**Figure 22:** Traffic on edges in the final iterations of simulations (23) and (24)

# CHAPTER V

# MODELING AND SIMULATING AIRSPACE DEGRADATION

## *5.1 Modeling the impact of weather perturbations on the airspace*

### 5.1.1 Weather Blockages

Weather has a major impact on the capacity of an airspace [23,33]. Weather blockages are a constant reality within the NAS. Often times they are the result of convective weather systems that pose a danger to aircraft, or make for bumpy and uncomfortable trips. In both cases, poor weather can prompt pilots to fly around any blockages. For this research, to establish if a weather blockage exists according to radar or forecasts maps, the vertically integrated liquid (VIL) is checked. VIL is the integration of reflectivity within a column of air. Typically, the higher the VIL means greater precipitation. The standard here is to check if the VIL ever surpasses a value of 3. Several studies from the literature [21,22,30] have shown that pilots are often unlikely to fly through weather above this threshold. In these cases, the area is considered blocked. By generating a number of polygons, the weather blockages can be represented mathematically.

In the continuity of the topics developed, a data-based approach is adopted. The impact of weather on traffic has been studied by Krozel et al. [16], by populating the airspace with obstacles according to a specific distribution. The work presented in this chapter incorporates the data-based model developed by previous research [6,29]. The weather polygons were computed on the same set of data, identifying weather

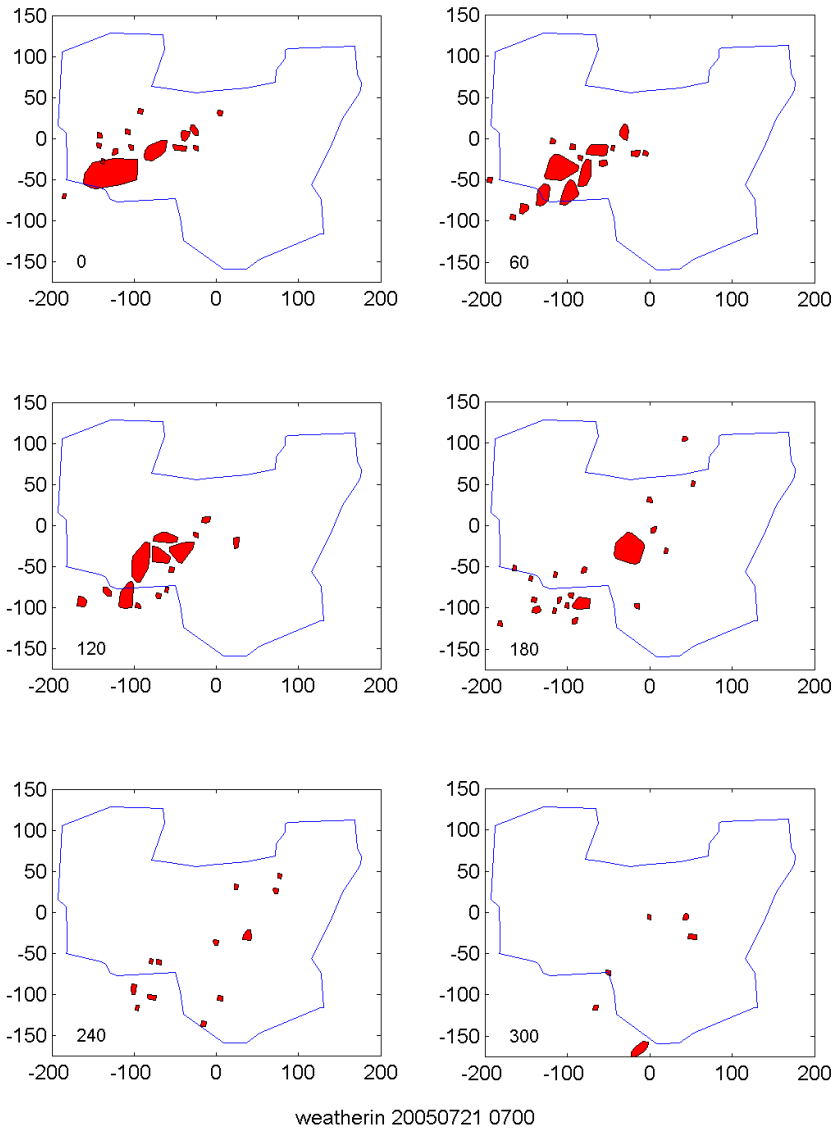


**Figure 23:** Map of the repartition of the polygons of weather for day 109, in the Cleveland center, for each of the six hours of the perturbation.

perturbations from May to August 2005 on the Cleveland center. For the purpose of the present work, two specific days were chosen for further research : July 21st and 24th 2005, days 109 and 112 in our data set. The weather perturbations on day 109 occurred from 07:00 am to 02:00 pm, and on day 112 from 11:00 am to 5:00pm, as

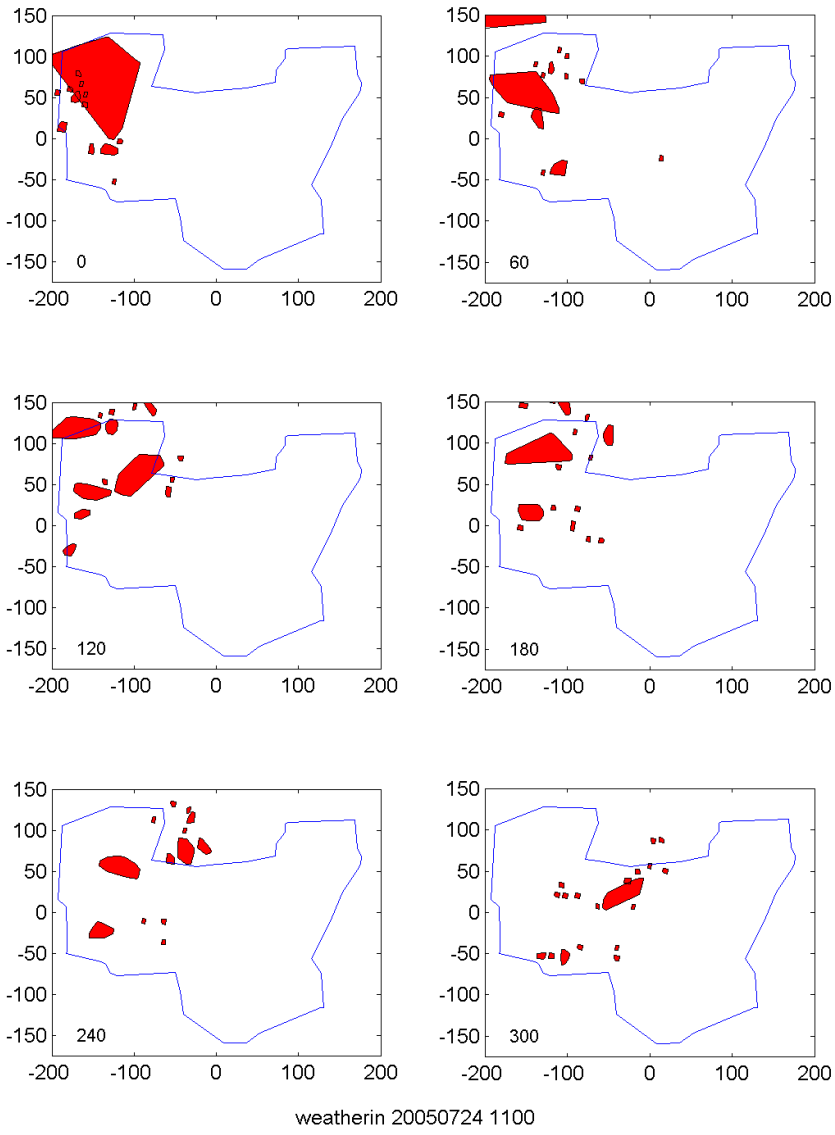


**Figure 24:** Map of the repartition of the polygons of weather for day 112, in the Cleveland center, for each of the six hours of the perturbation.

depicted in Figures 23 and 24.

### 5.1.2 Residual networks

The two scenarios of weather perturbations chosen correspond to the worst observed on the data set. They correspond to severe degradation of the airspace where they occur. Therefore, it is assumed that the share of the airspace overlapping the weather polygons is completely closed, at any altitude. A "discrete" approach is adopted, meaning that the network is considered static for each hour for which the polygons are set. While a dynamic approach might be considered, there is not sufficient data to support such a method. Indeed, weather data with a much shorter time horizon would be needed.

To compute the residual networks for each scenario and each time interval, the intersections between the edges of the network and the weather polygons are calculated. It is unnecessary to look for the edges that may be contained in a polygon (some of them are large), since they will be disconnected in any case. Figure 5.1.2 for day 109 and Figure 5.1.2 for day 112 represent the different residual networks at the different hours of the perturbations. The red edges are the edges impacted by the perturbation, the blue edges are not impacted and constitute the residual network, the polygons are represented in yellow.

Overall, a significant share of the network is impacted. As shown in Figures 27(a) and 27(b), up to 14% of the network edges may be cut, and more are hence disconnected from the network. However, as seen further, not only does the number of edges removed matter, but also does their importance relative to the connectivity of the network.

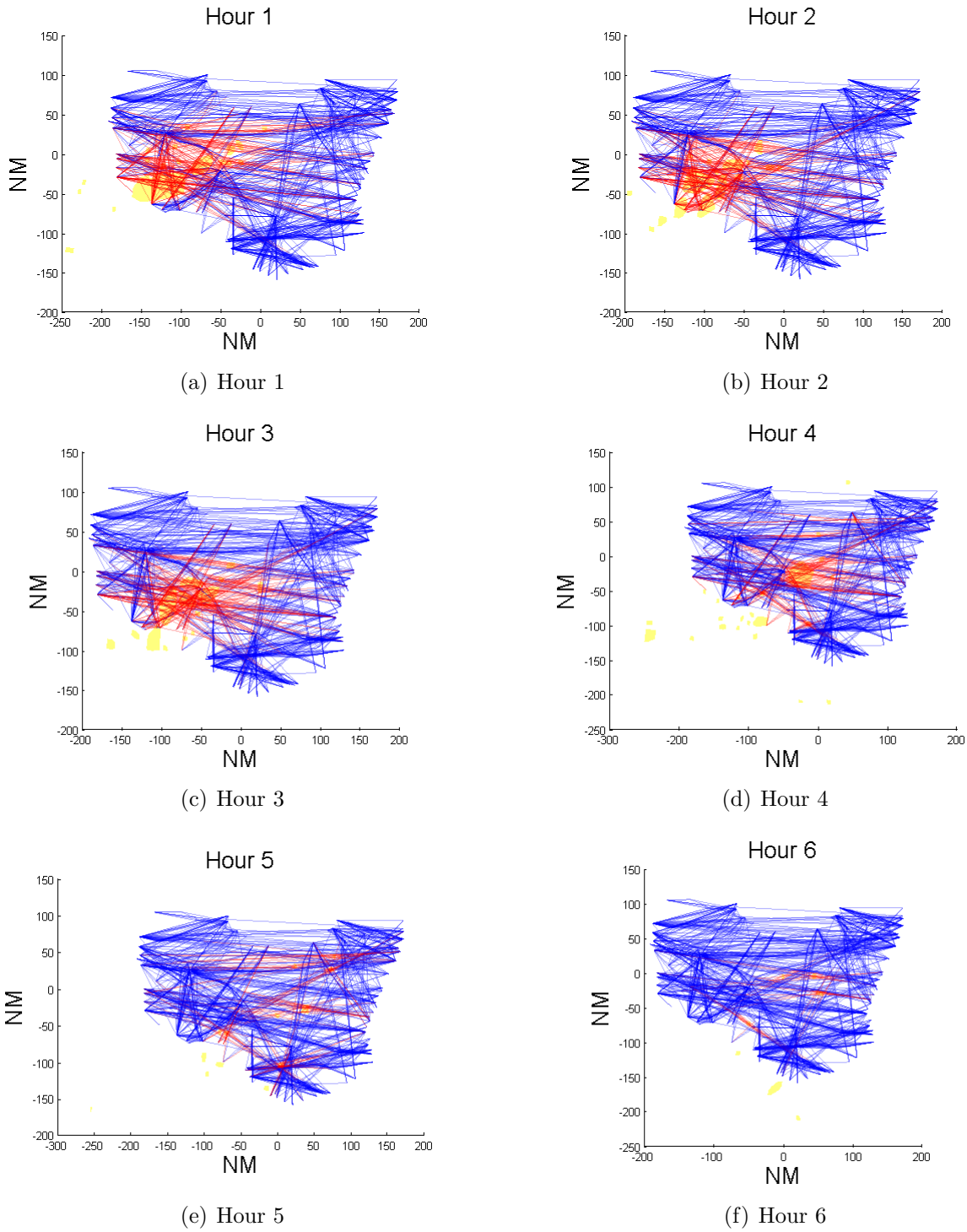


(a) Hour 1

(b) Hour 2

(c) Hour 3

(d) Hour 4

(e) Hour 5

(f) Hour 6

**Figure 25:** Weather perturbation on day 109, from 7:00 am to 1:00 pm: residual network in blue, edges removed in red, polygons of weather in yellow.

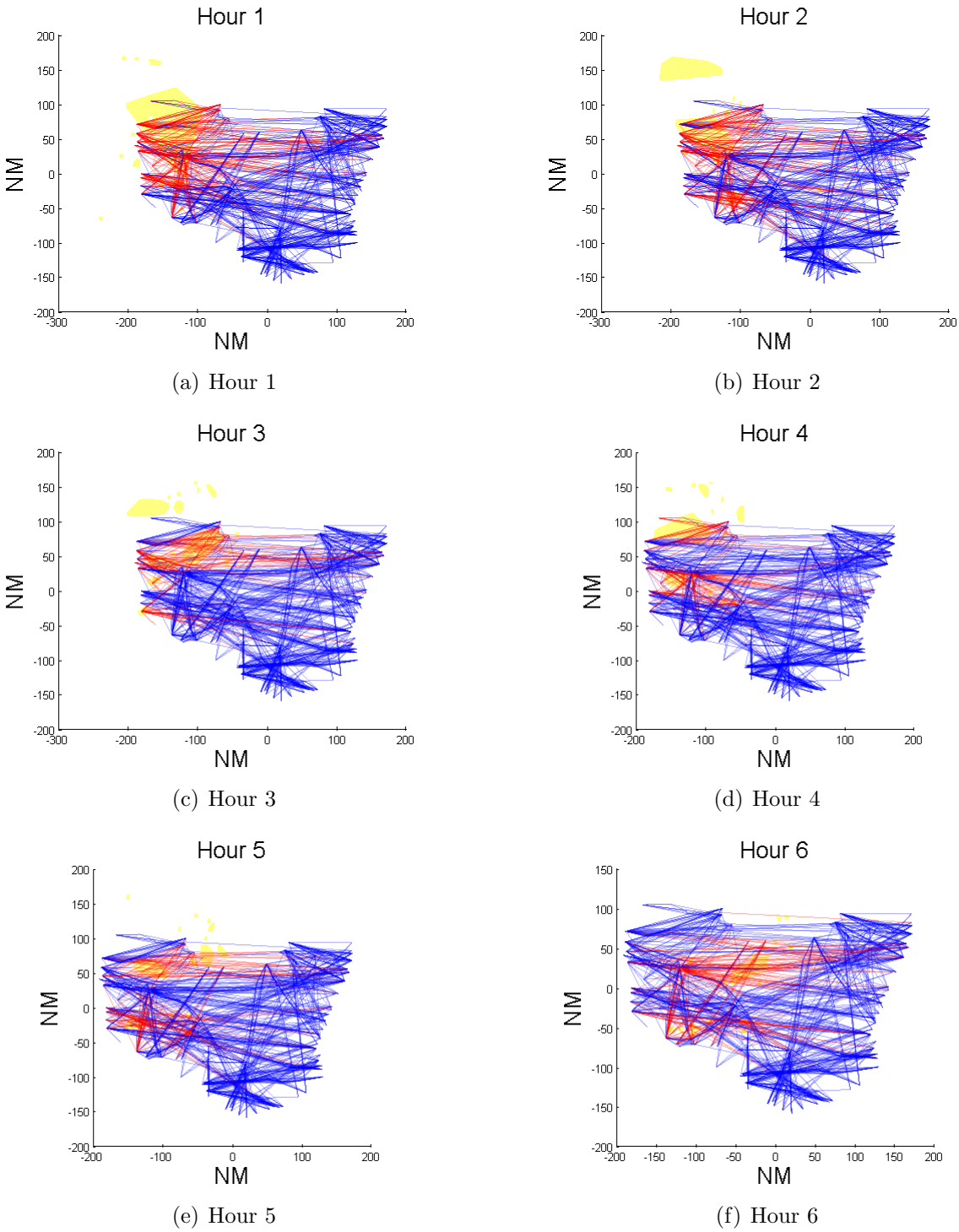


(a) Hour 1

(b) Hour 2

(c) Hour 3

(d) Hour 4

(e) Hour 5

(f) Hour 6

**Figure 26:** Weather perturbation on day 112, from 11:00 am to 5:00 pm: residual network in blue, edges removed in red, polygons of weather in yellow

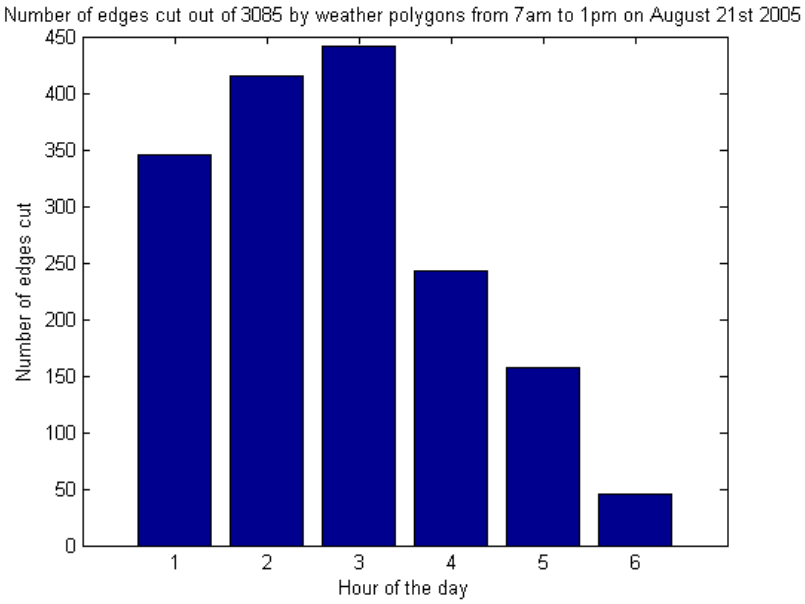


(a) Number of edges affected by the weather perturbation, for each hour, on day 109.

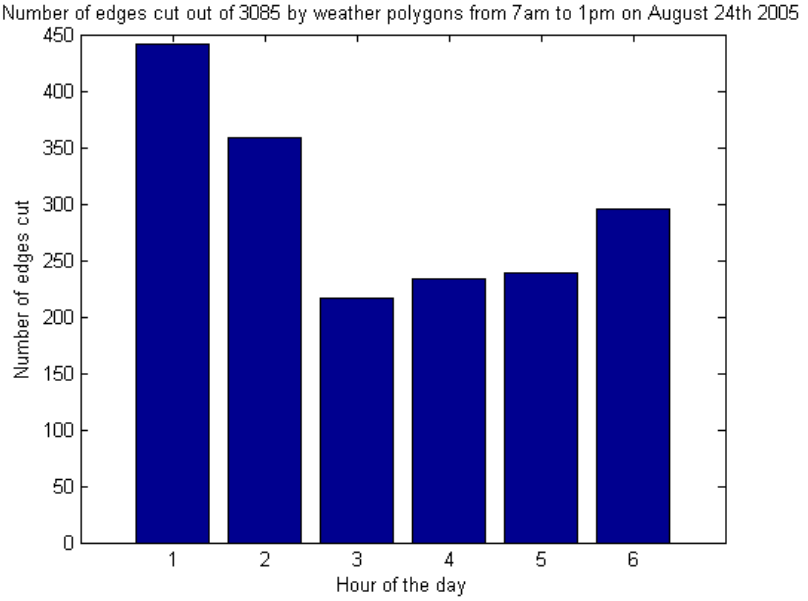


(b) Number of edges affected by the weather perturbation, for each hour, on day 112.

## *5.2 Optimizing air traffic on a perturbed airspace*

This section aims at presenting the results of different optimization simulations of traffic on the airspace center encountering weather perturbations.

### 5.2.1 Maximizing the throughput on the residual networks

As in the results without perturbations, the maximum throughput of the airspace is evaluated. In the present case, it is done for each of the six hours of the perturbations on day 109, on the corresponding residual network, that is, by setting the value of the flow on the edges affected by the perturbations to zero. The set of edges impacted at hour$j$ is defined as $E_j$. The optimization presents itself as follows, for $j = 1 : 6$.

$$\begin{aligned} &\text{maximize } \textstyle\sum_{k\in\mathbf{C}} s_k \\ &\text{subject to :} \\ &\qquad x_{i\in E_j} = 0 \\ &\qquad flow\ constraints \\ &\qquad sector\ constraints \end{aligned} \tag{25}$$

The results of the three iterations from (25) are displayed in Figures 27(c), 27(d) and 27(e). The results of the six hours for the last iteration are shown on the network in Figure 28, where only the edges drawn are active. The yellow shapes correspond to the weather polygons. These results show that the traffic on the network heavily depends on what the residual network is. Indeed, the airspace at hours 1 to 4 is impacted by larger weather polygons than hours 5 to 6. The number of origin destination pairs occupied remains stable through each iteration and each hour. The number of edges occupied varies significantly from an hour to another, that is when the network changes, but is quite stable through each iteration. The throughput, however, is the same for each hour, and decreases exactly the same way through the iterations. These facts and the representation of traffic on the network shown in Figure 28 show that, to maximize the throughput, almost the same origin-destination pairs are used, because they encounter little perturbation and have few conflict areas

with other routes, making them suitable to maximize the throughput. Nevertheless, as in the no-weather scenario, these results are only of interest to give upper bounds on the capacity of this given airspace under different perturbation configurations, but do not represent realistic demand patterns.

### 5.2.2 Maximizing the throughput under a fixed demand pattern on the residual networks:

As in the no-weather scenario, simulations aiming at maximizing the center throughput under a fixed demand pattern and a relaxed demand pattern ($\pm$ 10%) were run on the residual networks for each of the six hours of interest of day 109. The patterns chosen were the same as above, as computed by the average over all days of data. Except for the 6th hour, where the polygons are much smaller than in the others, no solutions were found to these simulations. This highlights the fact that the residual network cannot accommodate "usual" demand patterns. Removing edges, or equivalently setting their flow rates to zero, removes some or all of the paths joining the origin and destination nodes of certain pairs.

### 5.2.3 Minimizing the total distance with the good weather days data on the residual networks:

The next simulations were run using the traffic data of specific days at the same hours. The traffic patterns of the specific days of bad weather (days 109 and 112, that is 21st and 24th of July 2005) were extracted, both in terms of flows and the corresponding edges traveled, and origin-destination pairs traveled. Then, to compare with good days in terms of weather, other days were selected to be analyzed. For day 109, days 95, 102, 116 and 123 were chosen, because we expected to find similarities in traffic for days corresponding to the same day of the week. For day 112, days 98 and 105 were selected, but no more because the data seemed incomplete on other days.

The first optimization aimed at minimizing the total distance traveled by the aircraft during the hours of interest, on the residual network corresponding to weather

patterns on day 109 for the six hours, while constraining the traffic to travel on the same edges as on a good weather day, and to be at least of the same magnitude. The length of edge $k \in \mathbf{E}$ is designated as $l_k$, and the origin-destination demand from the data day as $s(m, n, p)$ where $m \in \mathbf{C}$, the set of commodities, and $n = 1 : 4$, for each day of good weather tested, and $p = 1 : 6$ for each hour. This is formulated as

$$\begin{aligned} &\text{minimize } \textstyle\sum_{k \in \mathbf{E}} l_k x_k \\ &\text{subject to :} \\ &\qquad x_{i \in E_j} = 0 \\ &\qquad s_l >= s(m, n, p),\ \forall l \in \mathbf{C} \\ &\qquad flow\ constraints \\ &\qquad sector\ constraints. \end{aligned} \tag{26}$$

With the data of the four days of good weather, no solutions were found for most of the six hours (solutions were only ever found for the intervals were the polygons were very small). This showed that the residual networks were not able to accommodate the traffic observed during regular days. The constraints on the residual network, traffic patterns and amplitude are too hard.

### 5.2.4 Minimizing the total distance with the bad weather day data on the residual networks:

The next simulation aimed at checking whether the residual networks could accommodate traffic observed on the bad weather day. It minimizes the total distance traveled by aircraft on the residual network, while forcing the traffic to at least match that of day 109. Define $s_q^r$ where $r \in \mathbf{C}$ and $q = 1 : 6$ for each hour, the origin-destination pairs pattern for day 109. The problem is formulated as

$$
\begin{aligned}
&\text{minimize } \textstyle\sum_{k\in\mathbf{E}} l_k x_k \\
&\text{subject to :} \\
&\qquad x_{i\in E_j} = 0 \\
&\qquad \forall l \in \mathbf{C},\ s_l >= s_q^r \\
&\qquad flow\ constraints \\
&\qquad sector\ constraints.
\end{aligned}
\tag{27}
$$

Out of these simulations, only those corresponding to hours 5 and 6 which include small polygons exhibited a solution. This is surprising at first. The residual network was built from exhaustive data over all days and specific data of the bad day. It would be expected that this network would be able to accommodate the traffic of that specific day. However, the enforced constraints are very hard. The graph abstraction model, though elaborate, does not capture the continuous dynamics of the weather, but only some discrete aspect. At first glance, it may seem like the data shows aircraft traveling through the perturbations. It may also be that the polygons that delimit no-fly zone were computed a posteriori, and that, at the time, there was more uncertainty. Also, a few aircraft may have flown through small portions of the airspace englobed in the polygons.

### 5.2.5 Minimizing the distance traveled in the polygons

Another approach was adopted to obtain realistic results on how traffic behaved in an airspace under perturbations. In this simulation, aircraft are allowed to travel inside the polygons (inside heavy weather). However, the optimization aims at minimizing the distance traveled by aircraft on the edges impacted by the polygons, while ensuring that traffic is at least the traffic observed on the bad weather day, for each of the six hours. This simulation was run for days 109 and 112. Define $E_w$ the number of edges impacted by the polygons. It is formulated as

$$\text{minimize } \sum_{k \in \mathbf{E_w}} l_k x_k$$

$$\text{subject to :}$$

$$s_l >= s_q^r \; \forall l \in \mathbf{C} \tag{28}$$

$$flow\ constraints$$

$$sector\ constraints$$

The results of (28) for the selected bad weather days are displayed in different figures. The traffic on the network in the third iteration is shown in Figure 30 for day 109 and Figure 32 for day 112. The comparisons of the different parameters of interest between iterations are displayed in Figures 29(a), 29(b), 29(c), 29(d) for day 109 and Figures 31(a), 31(b), 31(c), 31(d) for day 112.

For day 109, the results show that the commodities occupancy remains almost stable through the iterations. This is expected, since the commodities occupancy exceeds what was observed on day 109, and at the same time, trying to minimize the distance traveled in the polygons means that the traffic on the commodities tends to be constrained. This is also why the throughput is relatively stable through each iteration, unlike other simulations. As long as the controller taskload bounds are met, the throughput is almost set by the commodities occupancy. However, the throughput varies from an hour to another, because it depends heavily on the commodity occupancy constraint, which is set by the data for each hour. However, the edges occupancy varies a little more through each iteration, since, for a given commodity, several paths may be available, among which some may interfere less with the polygons of weather. Yet, the edge occupancy is significantly different for each hour, since it directly depends on which commodity demand is set to be nonzero. Besides, the objective depends mostly on the residual network of each iteration. For hours 5 and 6, where the polygons are small, it is even possible to completely avoid traveling routes impacted by weather, since the objective is zero. Observing the network maps

of traffic, it is seen that most of the edges are not fully occupied, except, as above, those located north, that encounter few conflict areas.The active part of the network also varies depending on the shape and location of the weather polygons.

The solutions found are very different for day 112, which further supports the claim that the objective linked to the residual networks and demand patterns greatly influence the results. First, the objective, while depending on the residual network for each hour, also depends on the iteration. It may suggest that the solutions first found for no conflict scenario were such that any alteration on the bounds of the controller taskload would force to use more routes impacted by weather. The throughput, which depends on the traffic entering the center on the origin-destination pairs, varies in the same manner as the origin-destination pairs occupancy, even if the variations are small. The edges occupancy shows that, to be able to maintain the same objective through the different iterations, while taking into account potential conflicts, a spreading on the network is necessary. This is highlighted for hours 3 and 4. The network maps corroborate these interpretations, showing a network more occupied than usual. This is certainly also due to the spreading of the polygons on the airspace.

## *5.3 Comparison of the optimization results and the data*

In this subsection, the optimization results are compared with the data from the days of the weather perturbations occurrence.

The comparison is drawn between the results of the last optimization run. This simulation aims at minimizing the distance traveled along edges impacted by weather, while ensuring the traffic observed on the days in question, and the data available. Both days 109 and 112 are compared respectively with the data. Their throughput for each hour, and the network occupancy, estimated by the number of edges occupied, are examined. For the data, an edge is considered occupied if it was a segment of a

flow that was traveled. The results are depicted in Figures 33(a) and 33(b) for day 109, and 34(a) and 34(b) for day 112.

The results are, as above, different for each weather scenario. For day 109, the throughput estimated by the simulation is larger or equal than what was observed in the data. On average, the throughput from the simulation is 24.8% larger than in the data. Nevertheless, the number of edges occupied is significantly smaller, by 48% on average. This alone would suggest that the optimization finds better routes, that is, routes with fewer edges, with higher aircraft flow rates on such routes. Yet, this seems to depend on the scenario examined. Indeed, for day 112, although the throughput from data is higher than in the simulations, the network occupancy is not. Depending on the hour, the network appears more or less occupied than it was in the data, but overall, the simulations give on average a 156% higher occupancy than what was observed, which is much larger than the throughput difference.

It is clear that the throughput of an airspace is linked to the demand patterns to be met, the localization and the size of the weather perturbations. However, determining the exact link has not been completely answered yet. The comparison of demand patterns over the same hour on the same day of the week has not yet revealed significant features. Important variations can be observed. Yet, there seems to be an indicator of either congestion or, at least, disruptions in the airspace: the percentage of outliers in the traffic. The outliers, i.e. the trajectories that could not be clustered in a flow, mentioned in Chapter 2 were not accounted for in the model developed in this thesis. Figures 35(a) and 35(b) show a comparison of the number of outliers on the days studied (109 and 112) with weather perturbations, and the same days of the week in the data set without perturbations. These figures show that the number of outliers increases when the airspace undergoes a degradation. The percentage of outliers in the traffic, in this case, is more than the average 20%.

Other factors could explain the variations observed in the data set, but the data available is not precise enough to verify them. First, VIL measurements may not provide "sufficient information about the vertical structure and dynamics (growth and decay) of convective cells - information that is often visible to pilots as they fly- to define completely regions of convective weather that pilots wish to avoid" [30]. However, this could be improved by taking into accounts echo tops as well as VIL measurements, which would imply defining 3D regions of weather blockages, and not assume that any altitude is blocked. Besides, a VIL value above 3 does not always imply that it is unsafe to fly, it is only dangerous when it corresponds to convective weather. Second, the inter-sector influence could be a cause of variations, in the throughput particularly. The model proposed covers ten en-route sectors, and therefore incorporates their inter-influence. Yet, because weather perturbations travel, it may not be sufficient to capture the influence of neighboring centers, especially when the weather perturbations are as severe as the ones studied. Moreover, only the portion of trajectories inside the Cleveland center were clustered. This is why artificial entry nodes and exit nodes inside the center were created. Having access to flight plans and linking them to the trajectories taken could help us determine which flights were actually rerouted, and compare the results with our optimization scheme. Furthermore, planned demand patterns are unknown. Having access to the planned trajectories, and hence the planned demand patterns, could help us discriminate in the data set which days or hours experienced higher or lower traffic intensity and why. There may be a way to mitigate congestion by applying in advance the findings of complexity metrics to airspace capacity, particularly during weather perturbations. This would improve our comparison of data and simulations, that are mostly based on throughput evaluation and network occupancy in terms of edges and origin-destination pairs. Furthermore, some flexibility could be added to the model.

For instance, taking into account the height and width of the flows that were used to compute the edges could help see which flows are completely impacted by the weather. Some flows corresponding to high altitude eastbound or westbound traffic can be very large. Another solution could be to allow edges to be translated by 10NM for instance.

Overall, these findings show that the model offered gives reasonable results. Obtaining and processing more data and more precise data, over larger shares of the airspace, could deepen our understanding of air traffic operations and optimize it, especially under perturbed conditions.

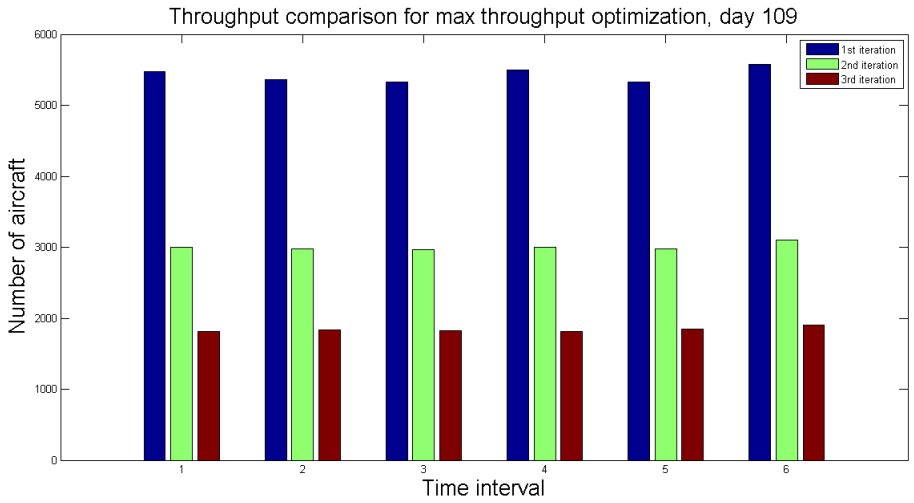


(c) Throughput at each iteration.

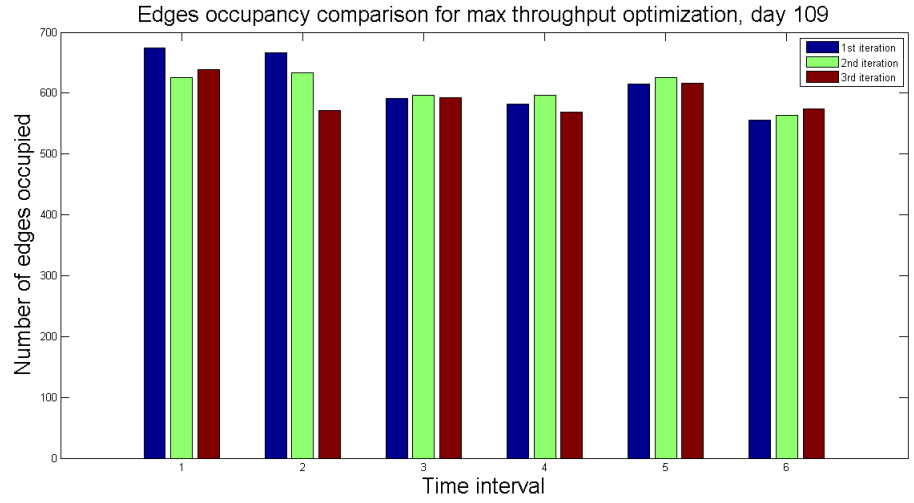


(d) Number of edges occupied at each iteration.

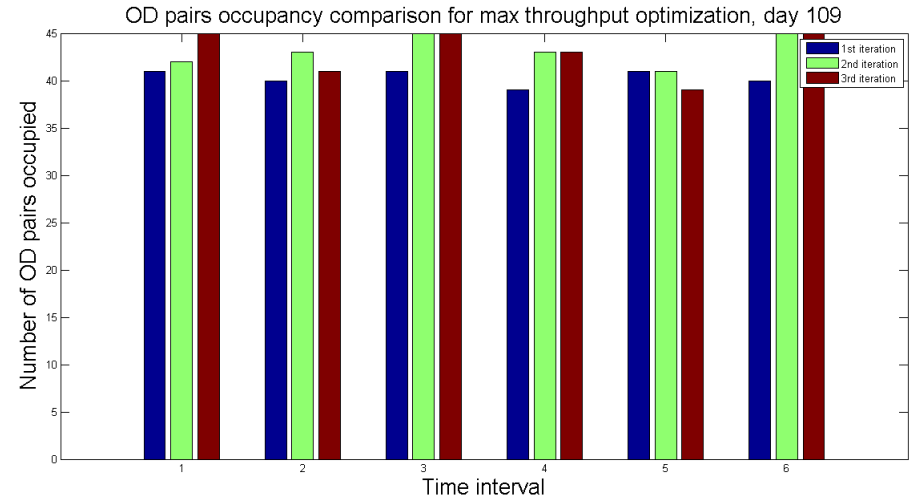


(e) Occupancy of Origin-destination Pairs at each iteration.

**Figure 27:** Results of the simulation corresponding to maximizing the throughput under weather perturbation (25)

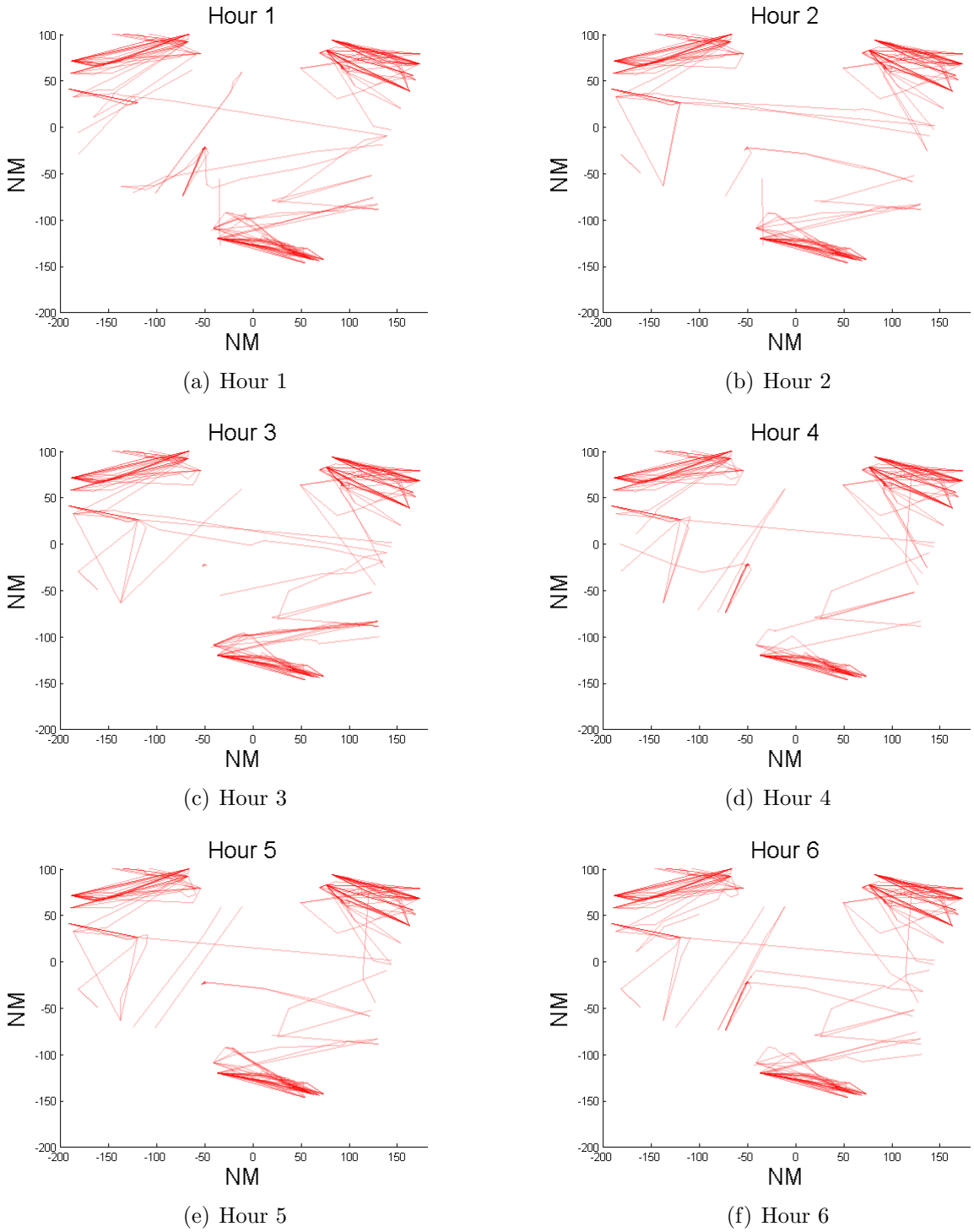


(a) Hour 1

(b) Hour 2

(c) Hour 3

(d) Hour 4

(e) Hour 5

(f) Hour 6

**Figure 28:** Traffic repartition on the network for the 3rd iteration of the simulation maximizing the throughput under weather perturbation (25)

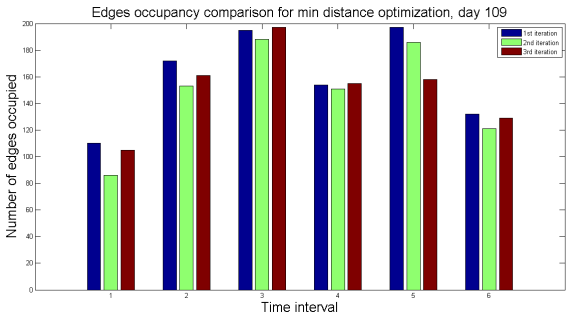


(a) Number of edges occupied at each hour

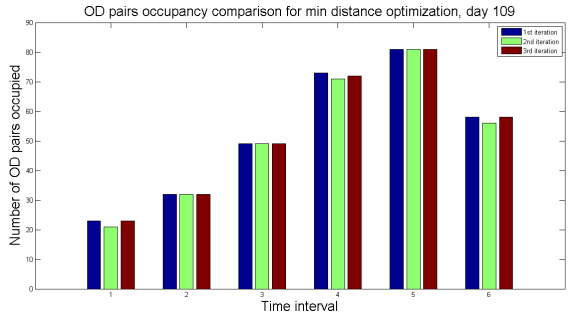


(b) Number of origin-destination pairs occupied at each hour

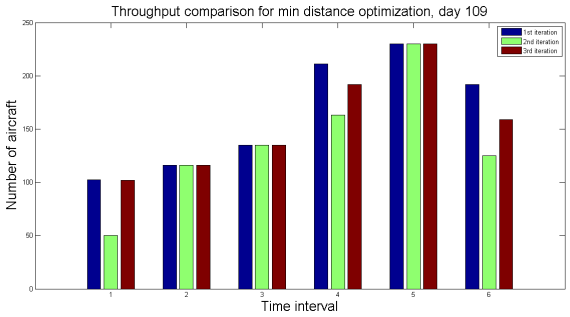


(c) Throughput at each hour.

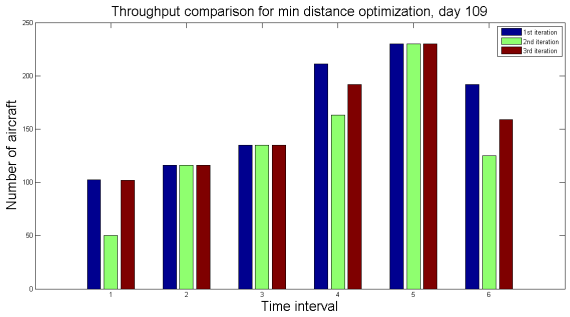


(d) Objective or Total Distance travelled by the aircraft inside the polygons at each hour.

**Figure 29:** Results of the simulation minimizing the distance travelled by aircraft inside the weather polygons (28) for day 109.

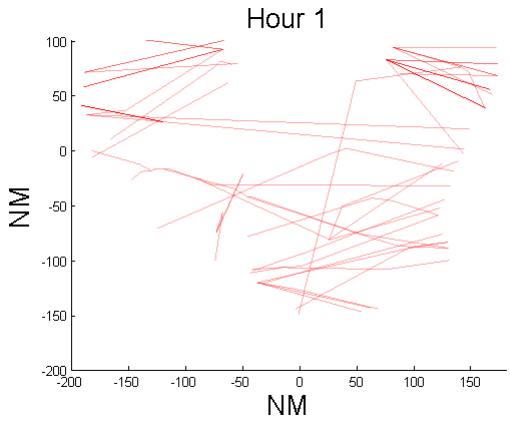


(a) Hour 1

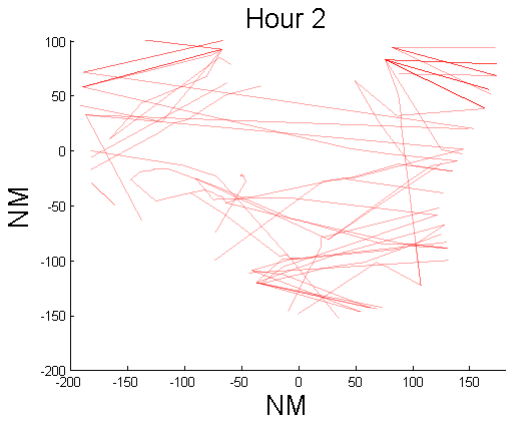


(b) Hour 2

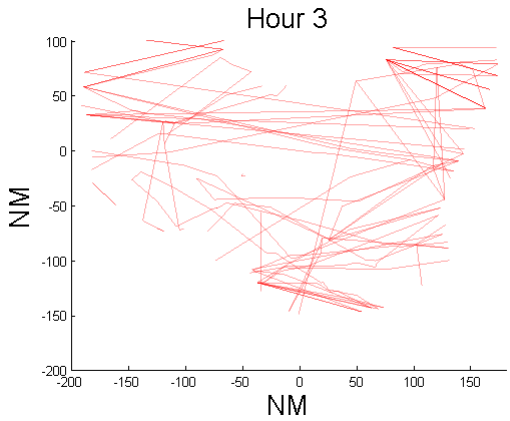


(c) Hour 3

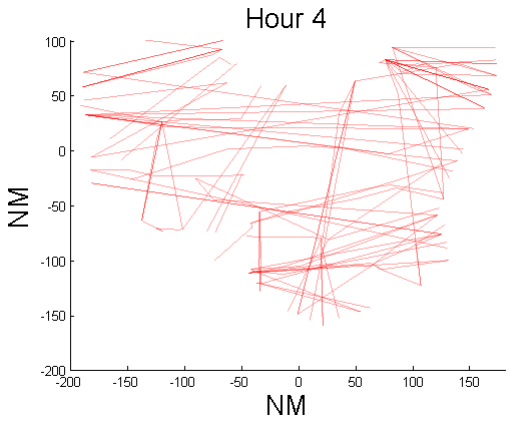


(d) Hour 4

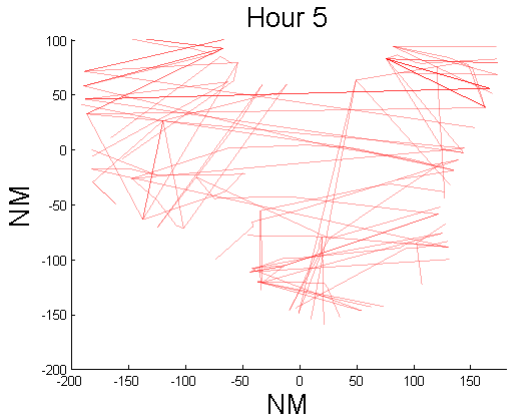


(e) Hour 5

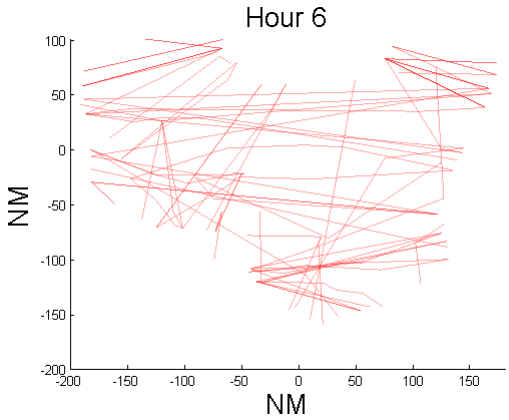


(f) Hour 6

**Figure 30:** Traffic repartition on the network at each hour, for the simulation minimizing the distance travelled by aircraft inside the weather polygons (28) for day 109.

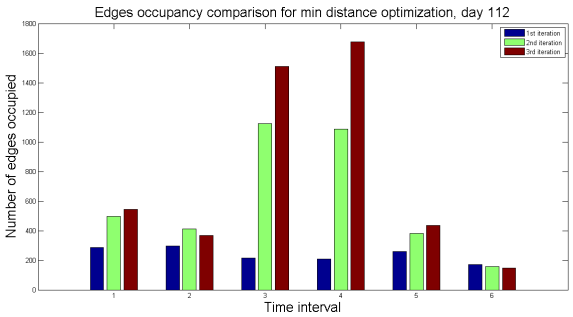


(a) Number of edges occupied at each hour

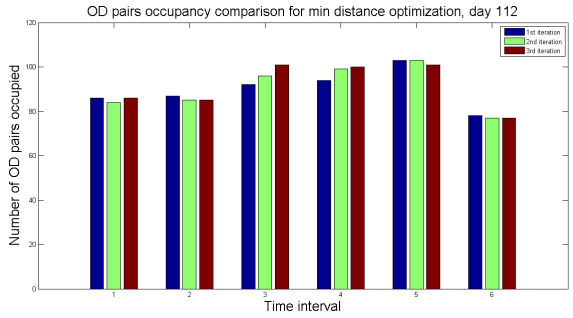


(b) Number of origin-destination pairs occupied at each hour

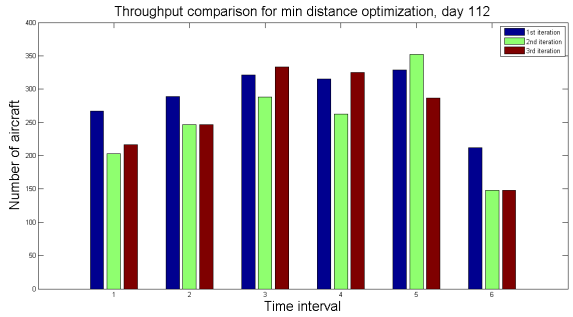


(c) Throughput at each hour.

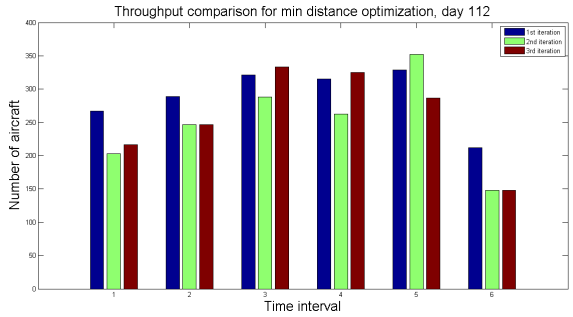


(d) Objective or Total Distance travelled by the aircraft inside the polygons at each hour.

**Figure 31:** Results of the simulation minimizing the distance travelled by aircraft inside the weather polygons (28) for day 112.

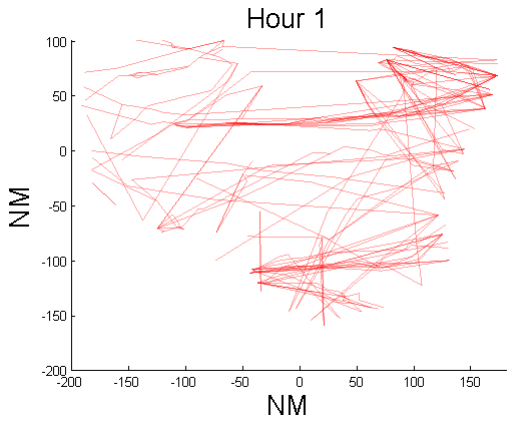


(a) Hour 1

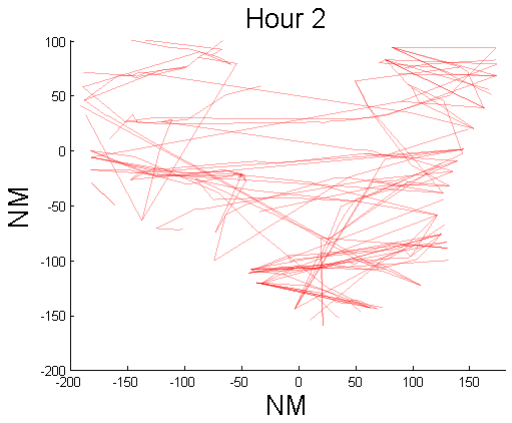


(b) Hour 2

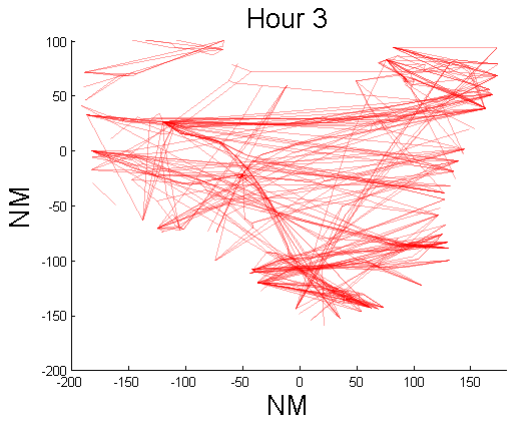


(c) Hour 3

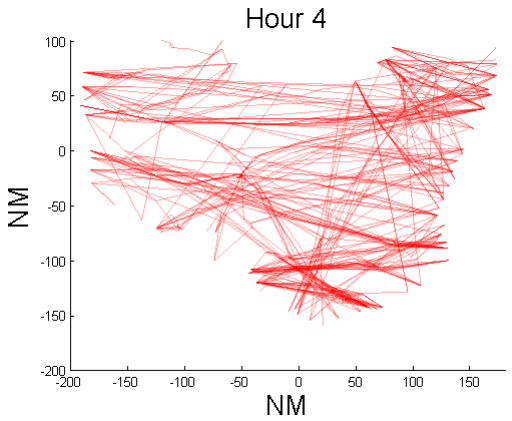


(d) Hour 4

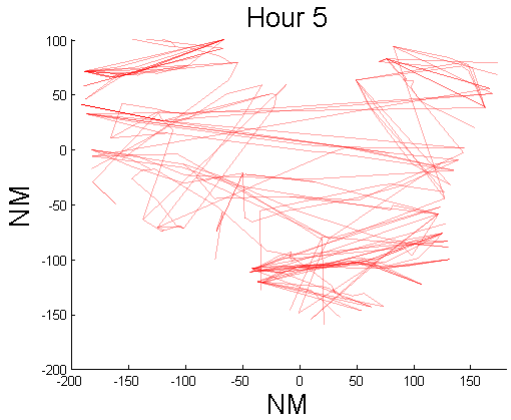


(e) Hour 5

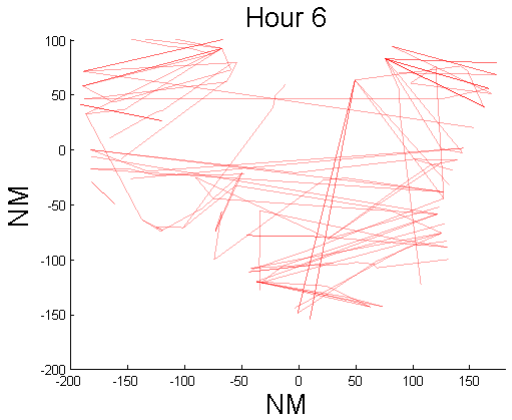


(f) Hour 6

**Figure 32:** Traffic repartition on the network at each hour, for the simulation minimizing the distance traveled by aircraft inside the weather polygons (28) for day 112.

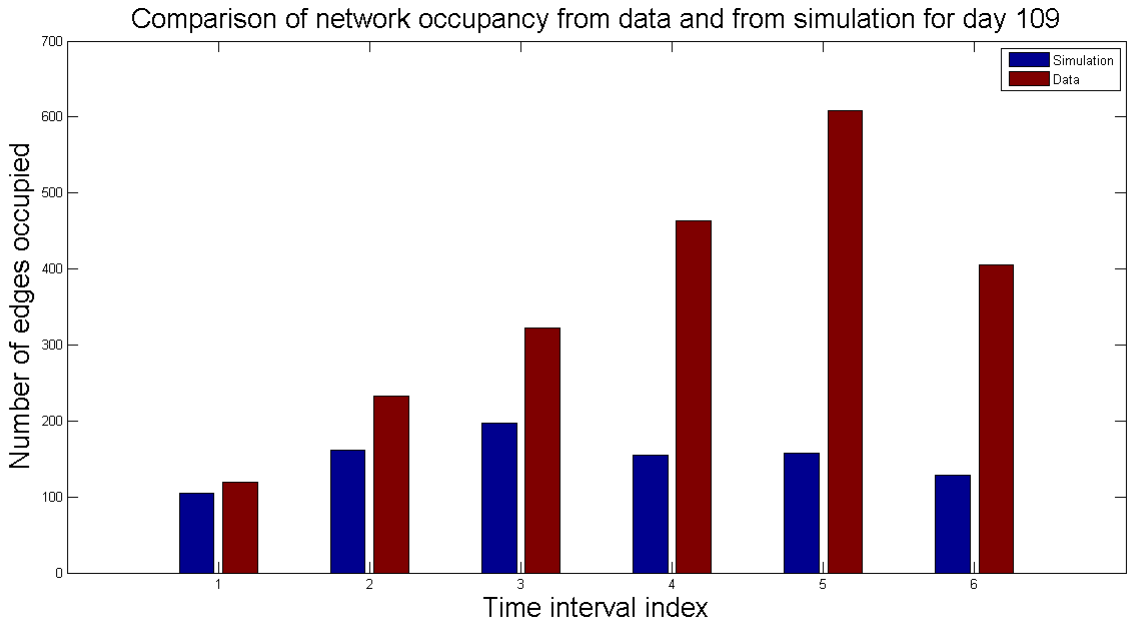


(a) Network occupancy comparison between data and simulation for day109.

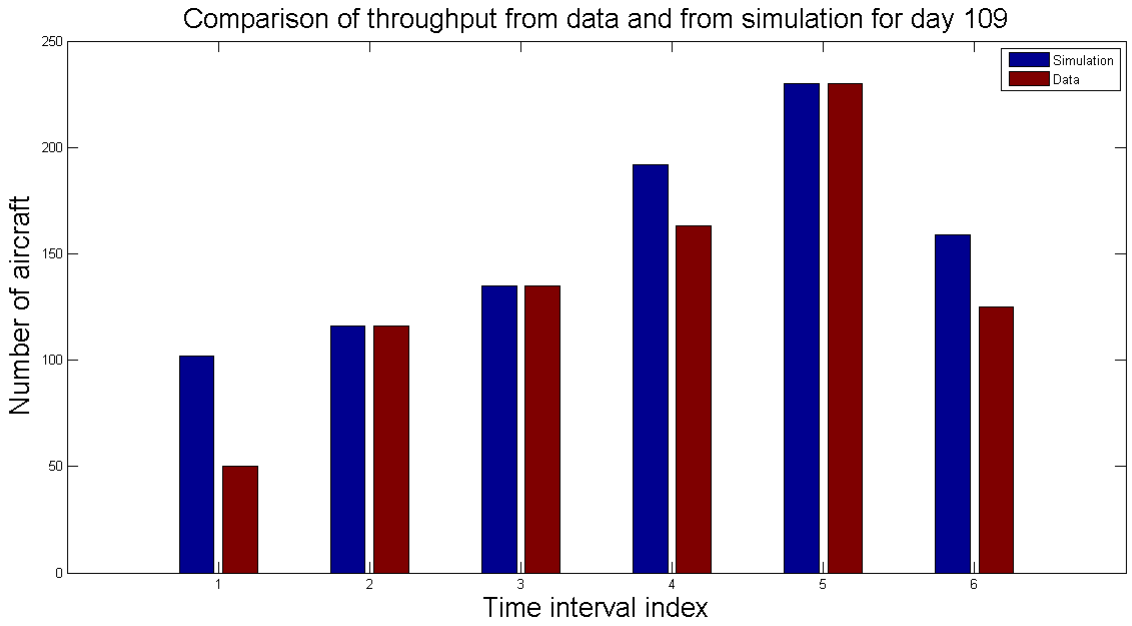


(b) Throughput comparison between data and simulation for day109.

**Figure 33:** Comparison of the data and the simulation results for the weather scenario of day 109.

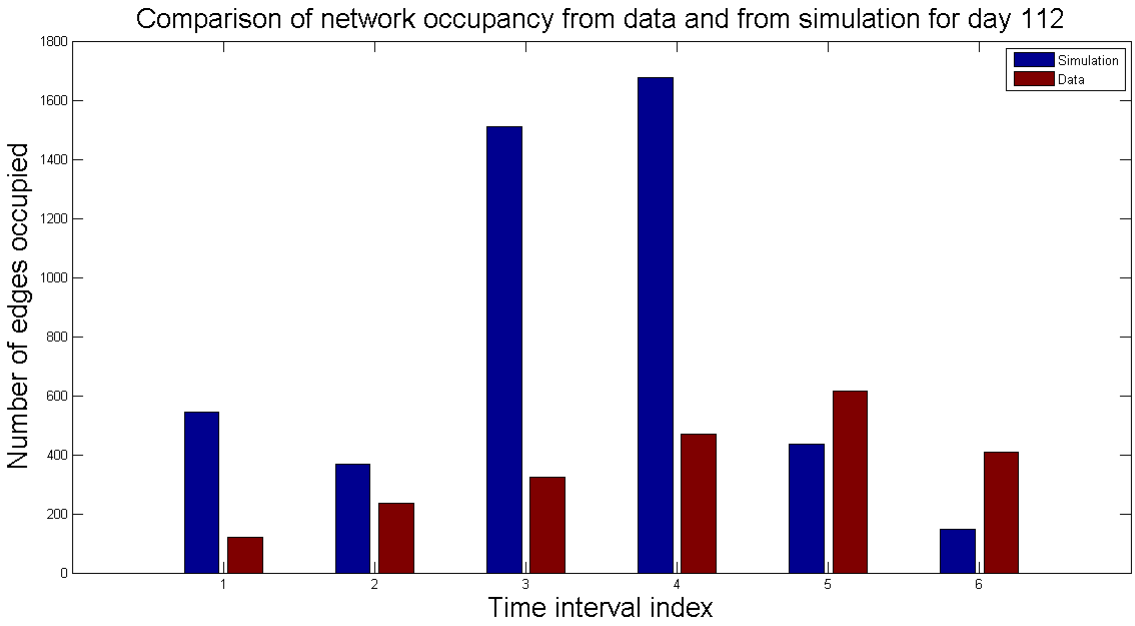


(a) Network occupancy comparison between data and simulation for day112.

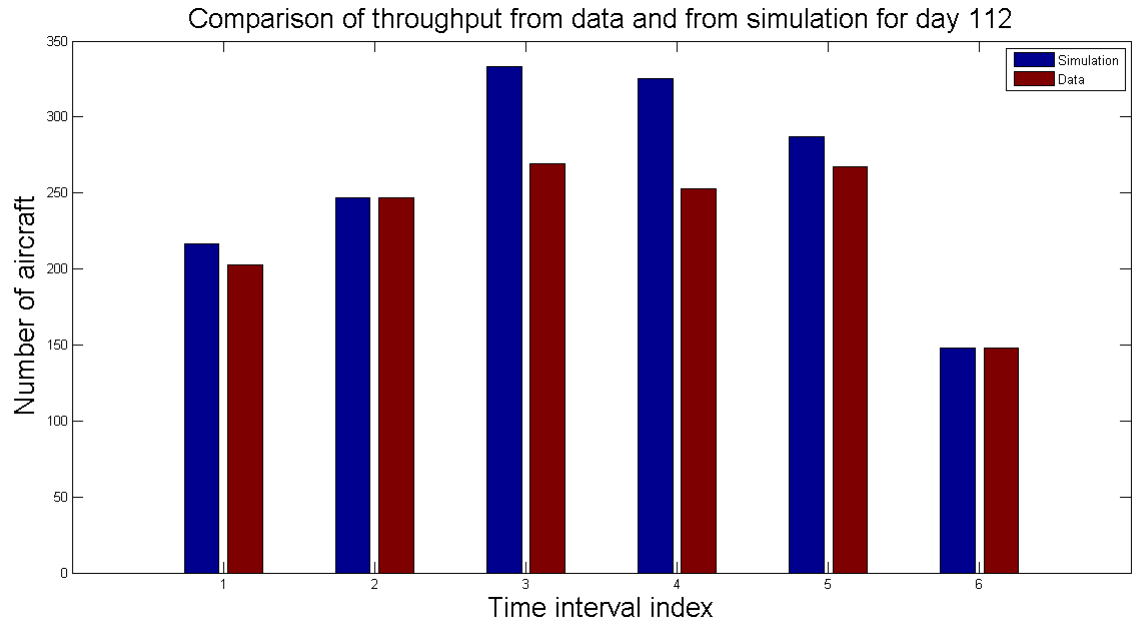


(b) Throughput comparison between data and simulation for day112.

**Figure 34:** Comparison of the data and the simulation results for the weather scenario of day 112.

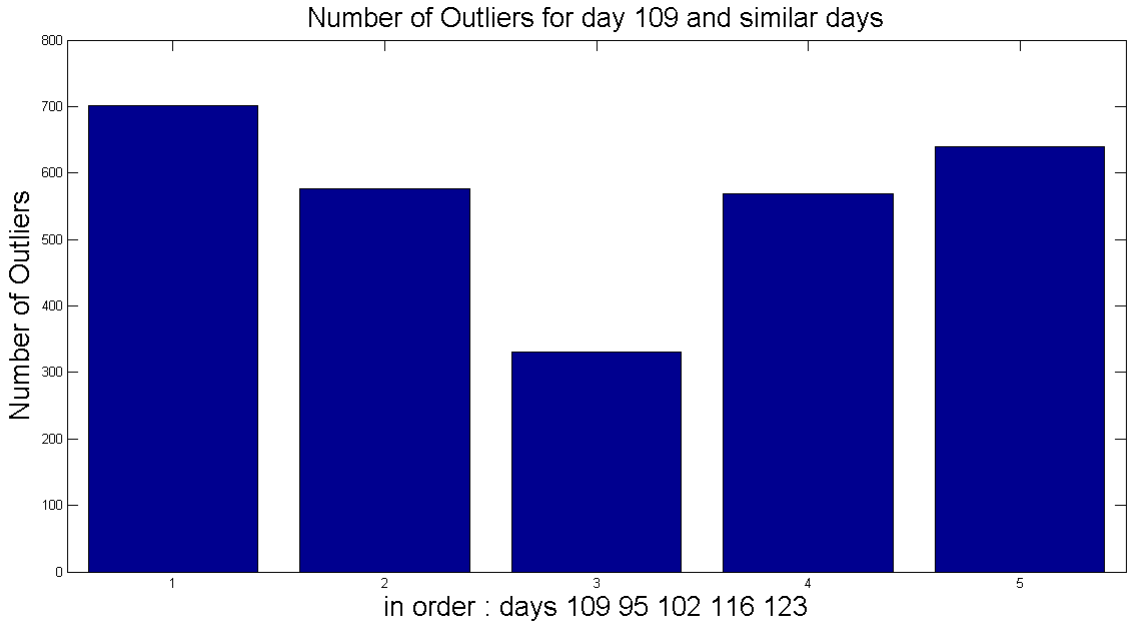


(a) Comparison of the number of outliers on the day 109, and similar days of the week

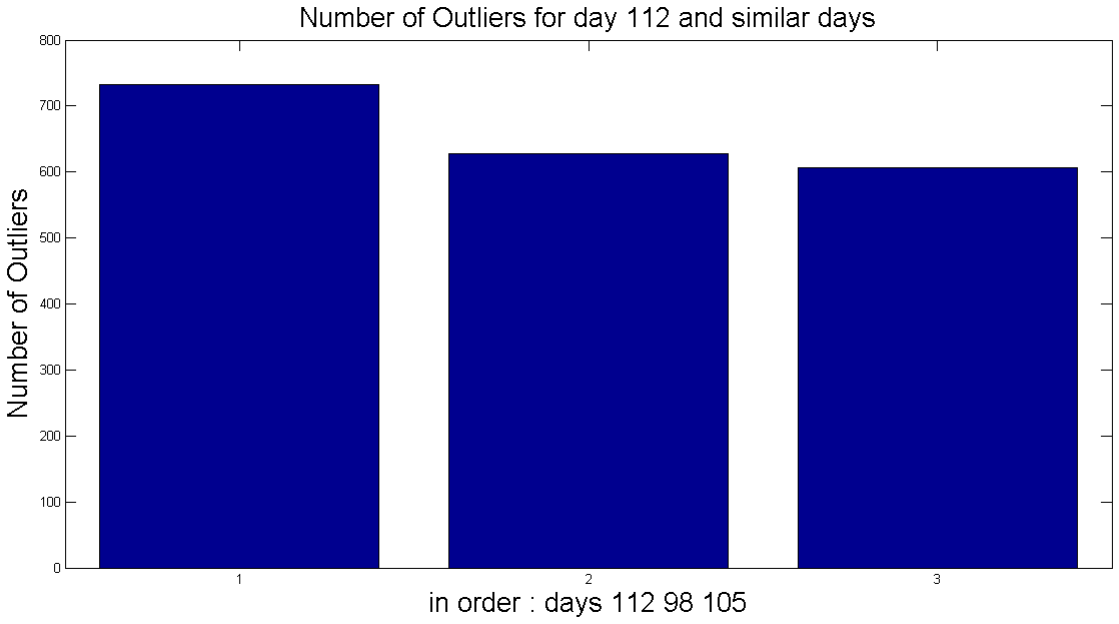


(b) Comparison of the number of outliers on the day 112, and similar days of the week

# CHAPTER VI

# CONCLUSION

## *6.1 Thesis summary*

This thesis aimed at developing a better understanding of how to analyze, model and simulate air traffic in a given airspace, under both nominal and degraded conditions.

First, a methodology to build a graph-abstraction of a given airspace from ETMS data was elaborated. No assumptions on the airspace were made when creating the 3D network flow model of the Cleveland center, as comprised of ten en-route sectors. Some parameters were chosen when using data-mining tools, mostly for computational reasons. From more than 300,000 trajectories collected over about 120 days, a directed graph with 1288 nodes was extracted. Only the origin-destination node pairs traveled in the data are considered. The re-routing options in this graph were explored.

Secondly, a general linear formulation for optimizing air traffic on the network is constructed. The aircraft are assumed to travel at constant speed in queues on the edges. New sector constraints are introduced, that are not based on aircraft counts contrary to the MAP parameter. These sector constraints try to make a precise use of the flow geometry in trying to estimate the controller taskload in a given sector, using results from complexity measures. The resulting formulation is computationally heavy but tractable. Simulations highlight the importance and the role of sector constraints and traffic demand patterns to estimate the throughput of a given airspace.

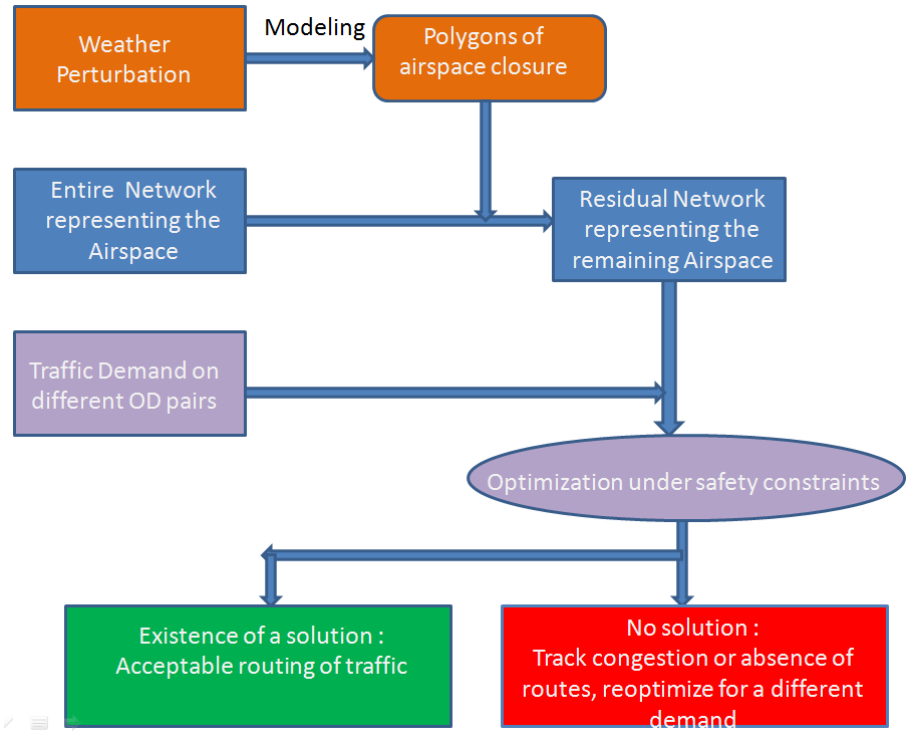


**Figure 35:** Modeling and Simulating Airspace Degradation.

Finally, weather perturbations scenarios are introduced. A previous modelization of weather perturbations as weather polygons is exploited, on the same data set as that of the ETMS data. The impact of these polygons on the network is analyzed. A quasi-static approach is adopted. Their influence is then simulated using the above optimization scheme. The results from these simulations are compared with the available data on the corresponding bad weather days. These results confirm the validity of the model and help point out further interesting research options.

On the whole, a traffic flow management framework for en-route traffic has been developed and tested under both nominal and perturbed conditions. The global approach is summarized in Figure 35. Few assumptions were made while constructing this approach. Because this research is data-based, it remains to assess whether the amount of data used is sufficient to extrapolate further. When building the network

or creating the linear constraints for the optimization, some parameters (such as the number of clusters, or the maximum flow rate of aircraft allowed on an edge) may be adapted to the case studied, depending on the level of precision wanted. The fact that the sector constraints are linked to the time-effort spent by the controller on the different tasks at hand and to the intrinsic flow geometry of each sector aims at estimating sector capacity better than the current MAP values.

## *6.2 Future work*

In this section are presented the various research leads emerging from the work achieved.

First, finding a shorter formulation for the problem presented should make it possible to model the entire National Airspace System (NAS), and optimize the traffic on it. ETMS data for a sufficiently large period could be gathered, and the methodology to make a network flow model applied. Clearly, the methodology adopted is applicable to any airspace. Nevertheless, some of the computational results depend heavily on the data observed.

Secondly, the current model is quasi-static. A given time interval is examined and the traffic repartition is solved for that interval, providing an acceptable solution or highlighting the presence of congestion, and calling for a re-evaluation. By transforming the model into a time-varying one, it could incorporate the potential delays. It would also help determine the emergence of congestion and watch its propagation, both under good weather and bad weather scenarios. The weather perturbations would also be time-varying and the weather modeling would be refined, to include echo tops for instance.

Furthermore, the model adopted is deterministic, and the addition of stochastic features could be a great benefit. It has been assumed that all aircraft were traveling on the edges computed from the flows. The outliers, i.e. the trajectories that were not clustered in the flows, have not been accounted for. This could be done by creating a flexible network, for instance. The outliers' presence is particularly observed in the data set during congestion or weather perturbations. Weather perturbations as blockages would be incorporated in the network formulation through morphisms acting on the graph according to relevant spatial and temporal correlations.

# REFERENCES


[1] A. Vela, E. Salaün, P. B. J.-P. C. and Feron., E., "Predicting controller communication time for capacity estimation," in International Conference on Research in Air Transportation, 2010.

[2] Bertsimas, D. and Patterson, S., "The air traffic flow management problem with enroute capacities," Operations Research, pp. 406–422, 1998.

[3] Bertsimas, D. and Patterson, S., "The traffic flow management rerouting problem in air traffic control: A dynamic network flow approach," Transportation Science, vol. 34, no. 3, pp. 239–255, 2000.

[4] Brooker, P., "Control workload, airspace capacity and future systems," Human Factors and Aerospace Safety, vol. 3, no. 1, pp. 1–23, 2003.

[5] Cardosi, K., "An analysis of en route controller-pilot voice communications," Tech. Rep. DOT/FAA/RD-93/11, US Department of Transportation, Federal Aviation Administration, 1993.

[6] Clarke, J., Solak, S., Chang, Y., Ren, L., and Vela, A., "Air traffic flow management in the presence of uncertainty," in Proceedings of the 8th USA/Europe Air Traffic Seminar (ATM09), 2009.

[7] Committee for a Review of the En Route Air Traffic Control Complexity and Workload Model, "Air Traffic Controller Staffing in the En Route Domain : A Review of the Federal Aviation Administrations Task Load Model," tech. rep., National Research Council of the National Academies, 2010.

[8] Corker, K., Gore, B., Fleming, K., and Lane, J., "Free flight and the context of control: Experiments and modeling to determine the impact of distributed air-ground air traffic management on safety and procedures," in Proc. of the 3rd Annual Eurocontrol International Symposium on Air Traffic Management, (Naples, Italy), 2000.

[9] Dell'Olmo, P. and Lulli, G., "A dynamic programming approach for the airport capacity allocation problem," IMA Journal of Management Mathematics, vol. 14, no. 3, p. 235, 2003.

[10] Gariel, M., "Toward a graceful degradation of air traffic management systems," 2010.

[11] Gariel, M., Srivastava, A., and Feron, E., "Trajectory clustering and an application to airspace monitoring," Arxiv preprint arXiv:1001.5007, 2010.

[12] Geng, R. and Cheng, P., "Dynamic air route open-close problem for airspace management," Tsinghua Science & Technology, vol. 12, no. 6, pp. 647–651, 2007.

[13] Grabbe, S. and Sridhar, B., "Modeling the aggregate distribution of flights in en route air traffic streams," AIAA Guidance, Navigation and Control Conference.

[14] Histon, J., Hansman, R., Aigoin, G., Delahaye, D., and Puechmorel, S., "Introducing structural considerations into complexity metrics," 2002.

[15] Histon, J., Hansman, R., Gottlieb, B., Kleinwaks, H., Yenson, S., Delahaye, D., and Puechmorel, S., "Structural considerations and cognitive complexity in air traffic control," in Digital Avionics Systems Conference, 2002. Proceedings. The 21st, vol. 1, pp. 1C2–1, IEEE, 2002.

[16] Krozel, J., Mitchell, J., Paakko, A., and Polishchuk, V., "Throughput/complexity tradeoffs for routing traffic in the presence of dynamic weather," in International Conference on Research in Air Transportation, 2010.

[17] Krozel, J., Penny, S., Prete, J., and Mitchell, J., "Comparison of algorithms for synthesizing weather avoidance routes in transition airspace," in AIAA Guidance, Navigation and Control Conf, 2004.

[18] Ky, P. and Miaillier, B., "Sesar: towards the new generation of air traffic management systems in europe," Journal of Air Traffic Control, vol. 48, no. 1, pp. 11–14, 2006.

[19] LULLI, G., "An integer optimization approach to large-scale air traffic flow management," Operations research, 2011.

[20] Manning, C., Mills, S., Fox, C., Pfleiderer, E., and Mogilka, H., "Using air traffic control taskload measure and communication events to predict subjective workload," tech. rep., Federal Aviation Administration, Office of Aerospace Medicine, 2002.

[21] Matthews, M. and DeLaura, R., "Evaluation of enroute convective weather avoidance models based on planned and observed flights," in 14th Conference on Aviation, Range, and Aerospace Meteorology (ARAM), Atlanta, GA, 2010.

[22] Matthews, M., Wolfson, M., DeLaura, R., Evans, J., Reiche, C., Balakrishnan, H., and Michalek, D., "Measuring the uncertainty of weather forecasts specific to air traffic management operations," in Aviation, Range, and Aerospace Meteorology Special Symposium on Weather-Air Traffic Management Integration, 2009.

[23] Mead, K., "Flight delays and cancellations," US Department of Transportation, Report Number CC-2000-356, 2000.

[24] Mitchell, J., Polishchuk, V., and Krozel, J., "Airspace throughput analysis considering stochastic weather," in AIAA Guidance, Navigation, and Control Conference, Citeseer, 2006.

[25] NextGen Integration and Implementation Office, "Nextgen implementation plan," in Federal Aviation Administration, 2009.

[26] Odoni, A., "Issues in air traffic flow management," Advanced Technologies for Air Traffic Flow Management, pp. 43–63, 1994.

[27] Porterfield, D., "Evaluating controller communication time as a measure of workload," International Journal of Aviation Psychology, vol. 7, no. 2, pp. 171–182, 1997.

[28] Prandini, M., Putta, V., and Hu, J., "A probabilistic measure of air traffic complexity in 3-d airspace," International Journal of Adaptive Control and Signal Processing, 2010.

[29] Ren, L., Chang, D., Solak, S., Clarke, J., Barnes, E., and Johnson, E., "Simulating air traffic blockage due to convective weather conditions," in Simulation Conference, 2007 Winter, pp. 1897–1904, IEEE, 2007.

[30] Rich DeLaura, M., "An exploratory study of modeling enroute pilot convective storm flight deviation behavior," in 12th Conference on Aviation Range and Aerospace Meteorology, 2006.

[31] Salaun, E., Gariel, M., Vela, A., Feron, E., and Clarke, J.-P., "Airspace statistical proximity maps based on data-driven flow modeling," AIAA Journal of Guidance, Control and Decision, to appear in 2011.

[32] Schmidt, D., "On the conflict frequency at air route intersections," Transportation Research, vol. 11, no. 5, pp. 351–355, 1977.

[33] Schumer, C. and Maloney, C., "Your flight has been delayed again: flight delays cost passengers, airlines, and the us economy billions," The US Senate Joint Economic Committee, 2008.

[34] Shingledecker, C. A., "Subsidiary radio communications tasks for workload assessment in R&D simulations," tech. rep., Air force aerospace medical research laboratory, 1982.

[35] Song, L., Greenbaum, D., and Wanke, C., "Predicting sector capacity for traffic flow management decision support," in 6 th AIAA Aviation Technology, Integration and Operations Conference, 2006.

[36] Song, L., Greenbaum, D., and Wanke, C., "The impact of severe weather on sector capacity," in 8th USA/Europe Air Traffic Management Research and Development Seminar (ATM2009), Napa, California, USA, 2009.

[37] Stein, E., Human Operator Workload in Air Traffic Control. New-York: Academic Press, 1998.

[38] Vela, A., Salaun, E., Gariel, M., Feron, E., Clarke, J., and Singhose, W., "Determining bounds on controller workload rates at an intersection," in American Control Conference (ACC), 2010, pp. 3063–3068, IEEE, 2010.